

N 67 8 2 5 5

NASA TECHNICAL
MEMORANDUM

NASA TM X-53630

June 30, 1967

NASA TM X-53630

INHOMOGENEOUS RADIANT HEAT TRANSFER FROM
SATURN ROCKET EXHAUST PLUMES

By Robert M. Huffaker
Aero-Astroynamics Laboratory

NASA

*George C. Marshall
Space Flight Center,
Huntsville, Alabama*

TECHNICAL MEMORANDUM X-53630

INHOMOGENEOUS RADIANT HEAT TRANSFER FROM SATURN ROCKET EXHAUST PLUMES

By

Robert M. Huffaker

George C. Marshall Space Flight Center

Huntsville, Alabama

ABSTRACT

A radiant heat transfer computer program has been developed to calculate radiation from inhomogeneous gases prevalent in rocket exhaust plumes from clustered engines. The infrared spectral absorption characteristics of the radiating species considered in this computer program - water vapor, carbon dioxide, carbon monoxide and carbon particles - have been determined. Band model parameters have been used to represent the infrared spectral absorption coefficients over 25 cm^{-1} increments. A modified Curtis-Godson approximation, used in the inhomogeneous heat transfer calculation, has been shown to give satisfactory results over the temperature and pressure range of interest in Saturn exhaust plumes. Results are shown for the Saturn-type engines for specific flow field assumptions. Some comparison with experimental spectroscopic data will also be presented. The effects of wavelength increment, field of view, and distance increment along the line of sight on the heat transfer, as well as the computer techniques for minimum computer time in calculating radiation from a three-dimensional flow field, are discussed.

NASA - GEORGE C. MARSHALL SPACE FLIGHT CENTER

NASA - GEORGE C. MARSHALL SPACE FLIGHT CENTER

Technical Memorandum X-53630

June 30, 1967

INHOMOGENEOUS RADIANT HEAT TRANSFER FROM SATURN ROCKET EXHAUST PLUMES

By

Robert M. Huffaker

PHYSICS SECTION
THERMAL ENVIRONMENT BRANCH
AEROPHYSICS DIVISION
AERO-ASTRODYNAMICS LABORATORY
RESEARCH AND DEVELOPMENT OPERATIONS

TABLE OF CONTENTS

	<u>Page</u>
I. INTRODUCTION.....	1
II. OUTLINE OF THE RADIATION PROGRAM.....	2
III. MSFC PLUME FLOW FIELD PROGRAM.....	3
IV. BAND MODELS.....	4
A. The Elsasser Model.....	6
B. Statistical Model.....	7
V. THE MODIFIED CURTIS-GODSON APPROXIMATION.....	8
VI. DETERMINATION OF THE BAND MODEL PARAMETERS.....	11
VII. RADIANCE CALCULATION FOR INHOMOGENEOUS ROCKET EXHAUSTS..	14
VIII. APPLICATIONS.....	17
IX. CONCLUSIONS.....	18

DEFINITION OF SYMBOLS

<u>Symbol</u>	<u>Definition</u>
$A(\bar{\nu})$	spectral absorptance
\bar{A}	average absorptance over a wave number interval
B_{ν}^0	Planck function
C	mole fraction of absorbing gas
d	spectral line spacing
D_b	band width
D	optical path
D_c	optical path for collision-broadened lines
D_D	optical path for Doppler-broadened lines
$f(X)$	Ladenberg-Reiche function
$K(\bar{\nu})$	spectral absorption coefficient
$K_{\lambda,C}$	carbon spectral absorption coefficient
ℓ	path length
ℓ'	hypothetical path in the Curtis-Godson approximation
P'_{ω}	temperature corrected pressure
P_T	total pressure
P_a^h	pressure of absorbing gas in the (homogeneous) h^{th} zone
P_b^h	pressure of foreign gas broadener in the (inhomogeneous) h^{th} zone
$P(S)$	intensity distribution function of a band radiant flux per unit area
\dot{Q}/A	radiant flux per unit area
S	spectral line intensity

DEFINITION OF SYMBOLS (Continued)

<u>Symbol</u>	<u>Definition</u>
\bar{S}	average line intensity over a finite wave number increment
S'	hypothetical intensity from an inhomogeneous gas for spectral lines
S^O	spectral line intensity per unit pressure
T	temperature in degrees Kelvin
T_O	reference temperature in degrees Kelvin
U	mass of gas per unit area
W	equivalent width
X	argument of Ladenberg-Reiche function
X'	argument of Ladenberg function in the Curtis-Godson approximation
Y_c	carbon mass fraction
γ	half-width of spectral line
$(\gamma_a^O)_h$	half-width of absorbing gas for homogeneous path
$(\gamma_b^O)_h$	half-width of foreign gas for homogeneous path
γ_c	band model collision-broadened half-width
γ_D	band model of Doppler-broadened half-width
λ	wave length
$\bar{\nu}$	wave number
θ, ϕ	angular spherical coordinates
σ_a	ratio of half-widths due to self-broadening
σ_b	ratio of foreign gas half-width to water half-width

DEFINITION OF SYMBOLS (Continued)

<u>Symbol</u>	<u>Definition</u>
$(\bar{\gamma}/d)_{\text{H}_2\text{O}}$	mean half-width to line spacing for water
$\tau(\bar{\nu})$	spectral transmittance
$\bar{\tau}$	average transmittance
τ'	inhomogeneous gas transmittance in the Curtis-Godson approximation

TECHNICAL MEMORANDUM X-53630

INHOMOGENEOUS RADIANT HEAT TRANSFER FROM SATURN ROCKET EXHAUST PLUMES

SUMMARY

A radiant heat transfer computer program has been developed to calculate radiation from inhomogeneous gases prevalent in rocket exhaust plumes from clustered engines. The infrared spectral absorption characteristics of the radiating species considered in this computer program - water vapor, carbon dioxide, carbon monoxide and carbon particles - have been determined. Band model parameters have been used to represent the infrared spectral absorption coefficients over 25 cm^{-1} increments. A modified Curtis-Godson approximation, used in the inhomogeneous heat transfer calculation, has been shown to give satisfactory results over the temperature and pressure range of interest in Saturn exhaust plumes. Results are shown for the Saturn-type engines for specific flow field assumptions. Some comparison with experimental spectroscopic data will also be presented. The effects of wavelength increment, field of view, and distance increment along the line of sight on the heat transfer, as well as the computer techniques for minimum computer time in calculating radiation from a three-dimensional flow field, are discussed.

I. INTRODUCTION

Heat transfer to the base of a launch vehicle can occur in two ways: by convection and radiation. Both of these modes are important especially on large vehicles which burn RP-1 (kerosene) and oxygen and on vehicles which burn hydrogen and oxygen. There is currently no completely satisfactory technique of calculating base heating for a given engine array at various altitudes and vehicle velocities. Therefore, both a better means of measuring heat transfer to the base region of vehicles actually under test and a more rigorous and reliable means of predicting heat transfer to vehicles before testing are required.

Convection to the base region depends upon the properties of the gas flow close to the surface being heated. For this type of heating, simple models of the flow, together with boundary layer correlations for the heat transfer coefficient, have been used in the past to arrive at local heating rates on the heat shield. Radiation, on the other hand, is sensitive to the entire flow field. Predictions have been made either by representing the exhaust plume as a surface with a given emissivity, temperature, and configuration, or by assuming a simple

geometrical configuration for the hot gas, which is presumed to be uniform, and integrating the equation of transfer with a simplified absorption coefficient.

The exhaust plume from a multiple-engine configuration like the Saturn V is an extremely complex gas-dynamical structure. The exhaust jets from the clustered engines interact with the atmosphere, and with each other, through an intricate series of shock waves and turbulent-mixing layers (figure 1). At the higher altitudes, on a multi-engined vehicle, the high-temperature, high-pressure collision zones between the engines can be a strong source of radiation (figures 2 and 3). Wherever the exhaust material that flows back into the base region mixes with the atmosphere, burning will occur; at low altitude, this burning is substantial. With such a complicated flow field controlling the heat transfer to a base region, it is not surprising that simple models of the heat transfer must be tied strongly to empirical data.

Helpful discussions with Mr. Werner K. Dahm on the radiative heat transfer problem and in the program definition are greatly appreciated. The cooperation of Mr. Robert Yossa, Mr. John Reardon and Mr. Marcus Dash is gratefully acknowledged, and assistance of Mr. Addison McGarrety in performing the computer programming is greatly appreciated.

II. OUTLINE OF THE RADIATION PROGRAM

In an effort to learn more about the base heating problem and to provide both mathematical techniques and values of parameters required for solution of the problem, a number of studies have been made both under contract and in-house at the Marshall Space Flight Center. These studies include the following:

(1) Determination of accurate flow fields, i.e., the temperature, pressure and concentration field of the exhaust plumes for single and multiple rocket engines.

(2) Accurate absorption coefficient data for the radiating species. This involves the determination of the band model parameters for the radiating species for the temperatures, pressures and concentration typical of Saturn V exhaust plumes. Water vapor, carbon dioxide, and solid carbon particles (soot) are the principal radiators in the first-stage plumes. Water vapor is the only radiator of importance in the plumes of the hydrogen-fueled stages. Extensive experimental and theoretical studies of the emission of CO_2 under various conditions have been made, and the properties of this molecule are well understood. Much less is known about H_2O .

(3) An exhaust plume radiation calculation program for inhomogeneous gases.

(4) Comparisons of calculated values with full scale radiation data.

III. MSFC PLUME FLOW FIELD PROGRAM

For first stage vehicles, the heating environment is determined from total and spectral radiation measurements in single engine exhaust plumes, and an empirical model developed, using a total emissivity in conjunction with a form factor program to calculate the radiation to the base. Because of the contribution of the afterburning layers, this calculated heat flux is at a maximum at sea level. This maximum value is used in the design of the heat shield. The plume radiation decreases as altitude increases, and the plume spreads, thus becoming cooler and less dense.

The upper stages of the Saturn V are powered by LH_2 -LOX engines, the Rocketdyne 200,000 lb thrust J-2. The S-II stage has a cluster of five J-2's, while the S-IVB has only one J-2. The radiation from the first stage engines is principally carbon, and is therefore continuum radiation; but the principal radiator in the upper stages is water vapor, with a band spectrum. The first stage design information obtained from experimental data on single engines is a relatively simple problem, but the design information on the upper stages must be entirely theoretical since scaling laws for model engine data are not yet known.

The chemistry of the LH_2 -LOX plume can be described if the appropriate thermodynamic properties and velocity can be solved simultaneously. The plume flow properties of the single engine on the S-IVB stage can be predicted with an axisymmetric method-of-characteristics program. To obtain flow properties in the intersecting plume region of the S-II stage, a three-dimensional program is needed. The gas plume in the intersection region radiates heat much more strongly than the undisturbed plume since the gas in the intersection region has crossed a shock wave, causing its temperature and pressure to rise. There are presently two efforts being funded which will result in programs to predict the flow in the plumes and intersection region of the S-II. One study uses a three-dimensional method-of-characteristics scheme. This scheme has the disadvantage of not being able to handle the imbedded subsonic regions which sometimes occur in the collision zones [2]. The other study uses a finite difference technique [4], which should be able to handle both subsonic and supersonic flow. All of the three-dimensional flow field work now being done is restricted to inviscid, non-reacting, constant gamma flows.

Equilibrium flow capability may be added later. The free shear layer is being neglected in the computation of radiation from the J-2 plumes.

The plume flow field work now being done by MSFC is summarized below. The items marked with asterisks are actually being used to furnish input to the radiation program; the other items should result in a better understanding of plume flow phenomena and will be used in other studies.

A. Single Nozzle

1. Inviscid Core

*a. Axisymmetric method-of-characteristics with either ideal gas or equilibrium.

b. One-dimensional gas-dynamic flow with equilibrium or finite rate chemistry for H_2-O_2 systems.

2. Nozzle boundary layer with mass injection and either ideal gas or equilibrium chemistry.

3. Turbulent free-shear layer with equilibrium chemistry for almost any gas, but finite rate chemistry for H_2-O_2 systems.

4. Multiple shock program.

5. Viscous far wake.

B. Clustered Nozzles

*1. Inviscid three-dimensional method-of-characteristics with ideal gas [2].

*2. Inviscid numerical finite difference scheme with ideal gas.

IV. BAND MODELS

If, in a specific wavelength region, the physical state of an absorbing or emitting gas is known, as well as the locations, intensities, and shapes of the lines, it is possible to calculate the radiation emitted by a specific sample of the gas. However, for the gases of interest in Saturn-type exhaust plumes, the absorption coefficient varies extremely rapidly with wavelength. Consequently, an exact calculation of the radiant heat transfer would be a formidable task even with modern computers. By using band models, it is possible to replace this detailed calculation over frequency by an average over selected frequency intervals.

Another objective of the use of a band model concept is to permit the interchange, in the heat transfer equation, of the order of integration over spatial and frequency variables. Band models may be said to have their origin in the theory advanced by Elsasser in 1938. For band models, in general, one begins by considering the equivalent width of a single line, defined by

$$W = \int A d\bar{\nu}, \quad (1)$$

where A is the absorptance. Assuming the Lorentz line shape, we have for the absorptance of a mass of gas, U , cm^{-2} ($= Pl$)

$$A = 1 - \exp[-K(\bar{\nu})U], \quad (2)$$

where

$$K(\bar{\nu}) = \frac{(S/\pi) \gamma}{(\bar{\nu} - \bar{\nu}_0)^2 + \gamma^2}. \quad (3)$$

S is the spectral line intensity defined by

$$S = \int_0^{\infty} K(\bar{\nu}) d\bar{\nu}, \quad (4)$$

and γ is the width of the line at half-maximum intensity. Integrating over all frequencies gives

$$W = 2\pi \gamma X e^{-X} [I_0(X) + I_1(X)], \quad (5)$$

where $I_0(X)$ and $I_1(X)$ are pure imaginary Bessel functions and $X = SU/2\pi\gamma$. The importance of the Ladenburg-Reiche solution - i.e., $W = 2\pi\gamma f(X)$ where $f(X) = Xe^{-X}[I_0(X) + I_1(X)]$ - is that the absorptance determined from the statistical band model can be expressed in terms of the characteristics of a single line. Also, any curve of growth (that is, a graph of W versus U) must have the shape of this function. By appropriate application of

the experimental data and the theoretical curve of growth, the parameters S/d and γ/d can be determined for a given pressure and path length.

Two useful models are the Elsasser and the random models. The latter was proposed by Mayer [5] and by Goody [6]. Sometimes the random Elsasser model is used, but this has been shown to reduce, ultimately, to the random statistical model.

A. The Elsasser Model

The Elsasser model assumes an infinite array of equally spaced, equally intense lines, all of which have the Lorentz shape. Since the array is infinite in extent, any line center ν_0 can be chosen as the center of the complete array. Thus, at a frequency ν , the absorption from a single line is

$$K\nu_1 = \frac{(S/\pi) \gamma}{(\bar{\nu} - 1d)^2 + \gamma^2}, \quad K\nu_2 = \frac{(S/\pi) \gamma}{(\bar{\nu} - 2d)^2 + \gamma^2}, \quad \dots, \quad K\nu_n = \frac{(S/\pi) \gamma}{(\bar{\nu} - nd)^2 + \gamma^2},$$

and the absorption at frequency ν from all the lines is then

$$K_\nu = \sum_{n=-\infty}^{n=\infty} \frac{(S/\pi) \gamma}{(\bar{\nu} - nd)^2 + \gamma^2}. \quad (6)$$

If we write $W = \bar{A}d$, since the absorptance over any portion of the band is the same as the absorption over a line, the formula

$$\bar{A} = 1 - \exp(-K_\nu U),$$

when integrated over $d\nu$, yields

$$\bar{A} = 1 - \frac{1}{2\pi} \int_{-\pi}^{+\pi} \exp \left[- \frac{SU}{d} \frac{\sinh \beta}{\cosh \beta - \cos 2Z} \right] dZ, \quad (7)$$

where $Z = \pi\nu/d$, and $\beta = 2\pi\gamma/d$. Two limiting cases of this integral are, in the weak-line approximation,

$$\bar{A}(\nu) = 1 - \exp(-\beta X),$$

and, in the strong-line approximation,

$$\bar{A}(\nu) = f(\pi\gamma SU/d^2), \quad (8)$$

where the right-hand side takes the form of an error function.

B. Statistical Model

The statistical model for a band assumes that the positions of the lines occur randomly and that the intensities of the lines in the band can be represented by some probability distribution function. The spectral transmittance, $\bar{\tau}$, is written in the form of Beer's law, and an average transmittance is written as

$$\bar{\tau} = \frac{\int_{\Delta\nu_1} \int_{\Delta\nu_2} \cdots \int_{\Delta\nu_i} \rho(\nu_1, \nu_2, \dots, \nu_i) d\nu_1 \dots d\nu_i \int_0^\infty \cdots \int_0^\infty \frac{n}{\pi} P(S_i) e^{-US_i} dS_i}{\int_{\Delta\nu_1} \cdots \int_{\Delta\nu_i} \rho(\nu_1, \nu_2, \dots, \nu_i) d\nu_1, d\nu_2 \dots d\nu_i \int_0^\infty \cdots \int_0^\infty \frac{n}{\pi} P(S_i) dS_i}$$

The argument of the exponential function contains the integrated intensity of a single line whose center frequency is situated at ν_i . In terms of the absorbance, this expression reduces to

$$\bar{A} = 1 - \left\{ 1 - D_b^{-1} \int_0^\infty W(S) P(S) dS \right\}^n. \quad (9)$$

But, since

$$\int_0^\infty W(S) P(S) dS$$

is the average value of the equivalent width for a single line, the absorptance is

$$\bar{A}(\bar{\nu}) = 1 - \exp[-\bar{W}/d], \quad (10)$$

where \bar{W}/d as a function of pressure and path length can be determined from a curve of growth at a particular temperature and over the particular wave number interval. Curves of growth, \bar{W}/d versus U , constructed from various probability intensity distribution functions $P(S)$ are shown in figure 4, and the corresponding absorptances are shown in table II. From figure 4, the maximum difference of \bar{W}/d for the curves of growth using a delta, exponential and a $1/S$ probability intensity distribution function is approximately 25 percent.

V. THE MODIFIED CURTIS-GODSON APPROXIMATION

To calculate the radiant heating from rocket exhaust plumes, we must know the spectral transmittances of the exhaust plume radiating gases. Since exhaust plumes are strongly inhomogeneous, we must determine the spectral transmittances of inhomogeneous gases in order to develop a calculation method. Under MSFC contract, a general method has now been developed to calculate spectral transmittances of inhomogeneous gases from the properties of homogeneous gases. Thus, any spectral transmittance for a particular inhomogeneous gas path can be calculated by properly combining known data on gases at constant temperature, pressure, and concentration [7].

The method developed is based principally on two special spectroscopic concepts: the molecular band model and the Curtis-Godson approximation. The band model yields an explicit closed formula for the molecular radiation within each selected spectral region of interest, which uses as input data the averaged line strength, the averaged line spacing, and the averaged line half-width. An average of 25 wave numbers is considered sufficient. The use of a band model is critically important for practical calculations of gas radiation. The Curtis-Godson approximation is a method of combining the parameters that appear in the band model formulae in such a way that the parameters needed for an inhomogeneous gas calculation are obtained solely from homogeneous gas data. This is a critical factor because the necessary parameters need be calculated or measured in the laboratory only for uniform gas samples. Without the Curtis-Godson or some equally good approximation, we would have to treat each inhomogeneous gas path as a special case. The band

model used was the random model with equal line intensities and equal line widths. In terms of the spectral transmittance, τ , at wave number, $\bar{\nu}$,

$$\ln \frac{1}{\tau} = 2\pi \frac{\gamma}{d} f(X), \quad (11)$$

where

$$X = \frac{(S/d) U}{2\pi(\gamma/d)}. \quad (12)$$

Since the Curtis-Godson method is based on the premise that one can substitute a hypothetical homogeneous path for an inhomogeneous path, this hypothetical path will have the same spectral transmittance as an inhomogeneous path if the parameters $(\gamma/d)'$ and X' as defined below are used in the band model formulae for the transmittance of a homogeneous gas.

If an inhomogeneous gas has a transmittance of τ' , then some hypothetical homogeneous sample has the same transmittance if it has certain values of $(\gamma/d)'$ and X' . The Curtis-Godson approximation gives us

$$\frac{S'}{d} \ell' = \sum_i \frac{S_i}{d} \ell_i = \sum_i X_i \frac{-\ln \tau_i}{f(X_i)} \quad (13)$$

and

$$\frac{S'}{d} \ell' \frac{\gamma'}{d} = \sum_i \frac{S_i}{d} \ell_i \frac{\gamma_i}{d} = \frac{1}{2\pi} \sum_i X_i \left[\frac{-\ln \tau_i}{f(X_i)} \right]^2, \quad (14)$$

which define the band model parameters of this particular homogeneous sample. The definition is given in terms of the band model parameters of the individual zones comprising the inhomogeneous path being studied; these zones are labeled with the subscript h .

$(\gamma/d)'$ is obtained by dividing equation (14) by equation (13).
 X' can then be determined by dividing equation (13) by $2\pi(\gamma'/d)$:

$$(\gamma/d)'_i = \frac{\sum_{h=1}^i P_a^h (S^0/d)_h \ell_h \left[(\gamma_a^0/d)_h P_a^h + (\gamma_b^0/d)_h P_b^h \right]}{\sum_{h=1}^i (S^0/d)_h P_a^h \ell_h} \quad (15)$$

$$X'_i = \frac{\left\{ \sum_{h=1}^i (S^0/d)_h P_a^h \ell_h \right\}^2}{2\pi \sum_{h=1}^i (S^0/d)_h P_a^h \ell_h \left[(\gamma_a^0/d)_h P_a^h + (\gamma_b^0/d)_h P_b^h \right]} \quad (16)$$

Substituting these values of $(\gamma/d)'_i$, X'_i into equation (11) yields an expression for the transmittance of the inhomogeneous path in terms of zonal transmittances and zonal X 's.

$$-\ln \tau' = \frac{\sum_i X_i \left[\frac{-\ln \tau_i}{f(X_i)} \right]^2}{\sum_i X_i \frac{-\ln \tau_i}{f(X_i)}} f \left[\frac{\left[\sum_i X_i \frac{-\ln \tau_i}{f(X_i)} \right]^2}{\sum_i \left[\frac{-\ln \tau_i}{f(X_i)} \right]^2} \right] \quad (17)$$

Generally, transmittances calculated with equation (17) are not very sensitive to errors in X_i . Therefore, with moderately accurate values of X_i , the accuracy with which τ' can be calculated is limited by the accuracy of the transmittance measurements and the suitability of the theory. This is particularly true in the high and low X regions where equation (17) reduces to a form in which τ' is independent of X_i . Thus, if all the X values are low (less than 0.2), $f(X) \approx X$, and equation (17) reduces to

$$-\ln \tau' \approx \left\{ \sum_i (-\ln \tau_i) \right\}. \quad (18)$$

If all the X_i 's are high (greater than 2.0), and $f(X) \approx (2X/\pi)^{1/2}$, equation (17) reduces to

$$-\ln \tau' \approx \left\{ \sum_i (-\ln \tau_i)^2 \right\}^{1/2}. \quad (19)$$

Equation (17), the general expression, can be used for any X values. Equations (18) and (19) are good in the low and high X regions, respectively. Experiments were carried out to test the Curtis-Godson theory for temperatures and pressures typical of rocket exhaust plumes. Band model parameters were measured for isothermal gases at various temperatures, the results were used to predict transmittances of known inhomogeneous paths, and the inhomogeneous path transmittances were compared to the theoretical prediction. Using a furnace-gas cell arrangement, numerous transmittances of water vapor inhomogeneous paths were measured and compared to transmittances calculated by the Curtis-Godson combination method in conjunction with the statistical band model. The results are shown in Tables III, IV, V, VI, and VII.

VI. DETERMINATION OF THE BAND MODEL PARAMETERS

Progress in the determination of the band model parameters and absorption characteristics for the radiating species in the Saturn-type exhaust plumes, H_2O , CO_2 , CO and carbon particles is described as follows:

1. H_2O

From the band model formulae, one can see that if values of $\bar{S}/d(T, \bar{\nu})$ and $\bar{\gamma}/d(T, \bar{\nu}, P_{\text{foreign gas}})$ can be determined, then the absorbance can be calculated for any $P\ell$. For thin-gas spectra where $(\bar{S}U/d)/(4\bar{\gamma}/d) \ll 1$, \bar{S}/d can be determined directly. A great many water vapor spectra over the wavelength range from 1 to 22μ , which have been published in recent years, cover the temperature range from $300^\circ K$ to $2700^\circ K$. The optical depths range between 0.2 and 100 cm-atm, and total pressures between 50 mm Hg and 10 atm. If sufficient thin-gas spectra at all temperatures were available, a set of $\bar{S}/d(T, \bar{\nu})$ values could be

derived directly. To obtain $\bar{S}/d(T, \bar{\nu})$ values from measured spectra in which the gas was not thin, the functional relationship between emissivity and optical depth must be known. The curve of growth given by the statistical band model has been used to determine the mean spectral absorption coefficients from thin and non-thin spectra by adjusting the fine structure term in such a way that the integral of the absorption coefficients over a given vibration rotation band results in the known value of the band intensity. Their values have been tabulated in reference 3. In general, the mean deviation of the $\bar{S}/d(T, \bar{\nu})$ values is within ± 20 percent (figures 5 and 6).

The average line spacing values, $d(T)$, obtained from the value of $\gamma/d(T, \bar{\nu})$ using the expression

$$\frac{\bar{\gamma}}{d}(\bar{\nu}) = \frac{\bar{\gamma}_{H_2O}^0}{d(\bar{\nu})} P_T \sqrt{T_0/T} \left[C(\sqrt{T_0/T} + \bar{\sigma}'_a) + (1 - C) \bar{\sigma}_b \right] \quad (20)$$

where

$$\bar{\sigma}'_a = \frac{\gamma_{H_2O}^{0'}}{\bar{\gamma}_{H_2O}^0},$$

and

$$\bar{\sigma}_b = \frac{\bar{\gamma}_b^0}{\bar{\gamma}_{H_2O}^0},$$

and where C is the mole fraction of water vapor. The value of $\bar{\gamma}_{H_2O}^0$ is $0.5 \text{ cm}^{-1} \text{ atm}^{-1}$ and $\bar{\sigma}' = 0.1$.

These results are shown in figure 7 along with the results of several other investigators. The straight line, a least squares fit, is given by

$$\bar{d}(T) = \exp[-.00106T + 1.21]. \quad (21)$$

These expressions for \bar{S}/d and $\bar{\gamma}/d$ were compared with the data of Simmons, Arnold and Smith [18]. (The results are shown in figure 8.) The above mentioned values of \bar{S}/d ($T, \bar{\nu}$) and $\bar{\gamma}/d$ ($T, P_{\text{foreign gas}}$) are now being used in the radiative heat transfer computer program. The values of $\bar{\gamma}/d$ for H_2O now in use do not take into account the wave number dependence. Since the $\bar{\gamma}/d$ values are determined from the asymptotic regions of the curves of growth [15], long path length measurements are required. Consequently, a long burner program was initiated to determine the necessary curves of growth. The design and fabrication of this burner have been completed under MSFC contract [3]. Measurements now in progress should be completed by November 1966. The long burner shown in figure 9 provides a homogeneous stable diffusion-controlled flame 2 inches wide and up to 30 feet long. Measurements will be made at pressures from .1 to 2 atm. with temperatures from 1300°K to 3000°K.

2. CO_2 , CO

The emissivity of these gases at high temperatures has been theoretically calculated by Malkmus [9,10] and by Thomson [11]. For CO_2 , many of these theoretical results have been verified by experiment [12, 13]. These calculations, which are believed to sufficiently represent the spectral properties of CO and CO_2 , have been described in detail in the original papers and are tabulated in reference 3. For CO, the calculated values of $(\bar{S}/d)_{STP}$ for the 4.6μ fundamental band are tabulated also in reference 3. For CO_2 , the values

$$(\bar{S}/d)_{STP}$$

and

$$\left[4 \frac{\gamma_o}{d} (\bar{S}/d)_{STP} \right]^{1/2}$$

for the 4.3μ fundamental band and the 2.7μ overtone band have also been tabulated, as a function of temperature and wave number. The agreement between the theoretical calculations of Malkmus and the experimental data of Oppenheim and Ben-Aryeh is reviewed in figure 10.

3. Carbon Particles

For LOX-RP engines, the dominant radiating constituent of the exhaust plume is carbon particles. For a heat transfer calculation, it was necessary to determine the absorption characteristics of this particular carbon found in rocket motors. The size of the carbon particles must also be known to determine the effect of scattering on the heat transfer. Studies were initiated to determine the emission

characteristics and size distribution of the carbon particles. The spectral emissivity of carbon clouds, produced at the exit plane of small rocket motors burning RP-1 and gaseous oxygen, was measured and compared with theoretical calculations. The rocket motors for this study used Foelsch-type nozzles. These nozzles produced an approximately constant temperature and velocity across the exit plane. The three motors used were with identical injectors, combustion chambers, and nozzle contours as far as the throat section. The diverging sections of the nozzles were different and expanded the combustion products to area ratios of 5.25, 3.0, and 1.5. In this manner, at a given mixture ratio and chamber pressure, carbon formed in a given amount under identical conditions was studied at three different temperatures. The product of the carbon mass fraction, Y_c , and the carbon cloud's spectral absorption coefficient, $K_{\lambda,c}$, has been determined for wave lengths between 1 and 4μ and temperatures between 1000 and 2600°K. The spectral dependence of $K_{\lambda,c}$, for temperatures below 1700°K, is in reasonably good agreement with the calculations of Stull and Plass [14] based on the D.C. conductivity of bulk graphite and appropriate to very small particles (figures 11 and 12). Setting $K_{\lambda,c}$ proportional to λ^{-1} and independent of temperature is also consistent with the present data below 1750°K. However, for temperatures above 1700°K, $K_{\lambda,c}$ appears to be almost independent of the wavelength. Apparent values of carbon mass fraction, determined from the combination of calculation and experiments, decreased very strongly with increasing O/F ratios and increased with increasing chamber pressure. The carbon particles have also been sampled in these small rocket motors and in a full-sized F-1 engine (see figure 18). Figure 13 indicates an approximate size of 400 Å, which agrees quite well with the calculations of Stull and Plass. We thus have the absorption coefficients for carbon particle clouds, and since the size of the particles is small compared to the wavelengths associated with the radiant energy in an exhaust plume, the effect of scattering on the heat transfer does not have to be considered.

VII. RADIANCE CALCULATION FOR INHOMOGENEOUS ROCKET EXHAUSTS

Two radiative heat transfer computer programs have been written to predict radiation from exhaust plumes. These programs differ only in geometric considerations, and the less complex of the two, which computes radiation from an axisymmetric exhaust plume, is described in this paper. The other program is similar but more geometrically complex because it was developed to calculate the radiation from a three-dimensional flow field such as that encountered with clustered rocket engines.

The computer programs use a modified Curtis-Godson approximation in the well-known radiative heat transfer equation. For purposes of calculation, the integral heat transfer equation is replaced by sums, over discrete locally homogeneous regions. The band model parameters used in these programs are over 25 cm^{-1} increments.

The geometry of the axisymmetric program is shown in figure 14. The left-hand coordinate system for the plume flow field has the Z-axis at the flow field centerline with +Z in the downstream direction. The X-Y plane corresponds to the origin of the flow field used (usually the nozzle exit), and the X-Y axes are oriented so that the point of interest is in the X-Z plane. The point of interest is the origin of a right-hand coordinate system with axes U, V, and W. The +W-axis is the outward normal to the surface of the unit area receiving radiation, and the U-axis is constructed to intersect the Z-axis at some point (this will be ∞ if the axes are parallel). The positive U direction is that given by a 90° clockwise rotation of the +W-axis when viewed from $Y = -\infty$.

Since the U-V plane coincides with the X-Z plane, the location and orientation of the point of interest are specified by Z and X coordinates and an angle of inclination ω . This inclination angle is measured clockwise when viewed from $V = -\infty$ between a vector \bar{V} parallel to and in the same direction as the +Z-axis and the +W-axis.

The spherical coordinate system used in computing the radiation has its origin at the point of interest. The line of sight, or radius vector, is ℓ , and θ is the angle between ℓ and the +W-axis. The angle between the projection of ℓ in the U-V plane and the +U-axis is ϕ .

To compute the radiation flux per unit area, \dot{Q}/A , the computer program uses constant values of $\Delta\theta$, $\Delta\phi$, $\Delta\bar{v}$, and $\Delta\ell$ between the prescribed initial and final values in evaluating the summation

$$\frac{\dot{Q}}{A} = \left\{ \sum_{\theta_i}^{\theta_f} \left[\sum_{\phi_i}^{\phi_f} \sum_{\bar{v}_i}^{\bar{v}_f} \sum_0^{\ell_f} - B_{\bar{v}}^0 (\tau_{\ell} - \tau_{\ell-\Delta\ell}) \right] \sin \theta \cos \theta \right\} \Delta\theta \Delta\phi \Delta\bar{v} . \quad (22)$$

The summation of the transmissivity, τ_{ℓ} , begins with $\tau_{\ell=0} = 1$ and in subsequent increments uses

$$\tau_{\ell} = \exp \left(- \sum_0^{\ell} D \right) , \quad (23)$$

where the optical path, D , taking into account both Doppler- and collision-broadening, is given by

$$\sum_0^l D = \sum_0^l F \left\{ 1 - \left\{ \left[1 - \left(\frac{\sum_0^l D_c}{\sum_0^l F} \right)^2 \right]^{-2} + \left[1 - \left(\frac{\sum_0^l D_D}{\sum_0^l F} \right)^2 \right]^{-2} - 1 \right\}^{-1/2} \right\}^{1/2} \quad (24)$$

and

$$F = \bar{K} P'_\omega \Delta\ell. \quad (25)$$

For collision-broadened lines,

$$\sum_0^l D_c = \sum_0^l F \left[1 + \frac{\left(\sum_0^l F \right)^2}{\sum_0^l \frac{\gamma_c}{d} F} \right]^{-1/2} \quad (26)$$

and for Doppler-broadened lines,

$$\sum_0^l D_D = \frac{1.7 \sum_0^l \frac{\bar{\gamma}_D}{d} F}{\sum_0^l F} \left\{ \ln \left[1 + \left(\frac{0.589 \left(\sum_0^l F \right)^2}{\sum_0^l \frac{\bar{\gamma}_D}{d} F} \right)^2 \right] \right\}^{1/2}. \quad (27)$$

At the center of each Δl increment along each line of sight, the position in the flow field is computed, and the properties at that point are determined from the tabulated flow field properties by linear interpolation. This provides an estimate of the pressure, P, temperature, T, and concentration, C, at that point, for use in the radiance calculation. The pressure is converted to a temperature-corrected partial pressure (actually a density ratio), using

$$p'_{\omega} = \frac{273}{T} (P/1 \text{ ATM}) C.$$

A table of absorption coefficients listed for the exact values of wavelength used in the program and several temperatures is used to determine the effective absorption coefficients by linear interpolation in temperature. The values of γ_c , γ_D , and $1/d$ are determined using relations listed in Table II. Now all of the values are available for evaluating a step in the inner summation of equation (22), and the procedure is repeated at the center of succeeding Δl increments until the maximum distance, l_f , is reached. To save time in searching the flow field, the inner sum of equation (22) is simultaneously evaluated for 300 wave number values. This is sufficient to cover the spectral range of interest in most problems so that each line of sight has to be traversed only one time.

To account for blockage of radiation along particular lines of sight by the engine nozzles and vehicle structure, the program has the capability of providing up to 50 "blocking circles." These can be located anywhere in the flow field in planes normal to the Z-axis and can be either a disk which would block lines of sight passing the plane within the circle or a hole which would block lines of sight passing the plane outside the circle. Using these blocking circles an engine contour can be approximated as a stack of "disks," and a structure such as an interstage skirt can be approximated as a stack of "holes."

VIII. APPLICATIONS

The radiation computer program results are now being compared with various radiation measurements; one of these comparisons for which preliminary results are available is described. The radiation measurement was made during a test of a duration model rocket at Cornell Aeronautical Laboratory.

The short duration rocket testing technique uses nonsteady flow techniques with gaseous propellants to provide steady flow model rocket firings on the order of 5 to 10 milliseconds. The short test time allows high altitude simulation and eliminates the need for nozzle cooling systems.

Short duration models of two F-1 engines (1/45 scale) were used in the radiation measurement program. The configuration of the models simulated the engine spacing between the center and outboard engines on the Saturn S-IC stage. The Warner and Swasey Model 501 fast-scanning spectrometer, which was used for making the spectral measurements, is capable of making a spectral scan in 1 millisecond with a 0.25 millisecond interval between scans. It uses two detectors, and the two channels of output are presented on oscilloscopes and photographed. Since there is no absolute wavelength reference in the data presentation, it must be fixed by the spectral features. Therefore, slight wavelength discrepancies in the comparisons presented should be interpreted as uncertainty in the data reduction rather than actual comparative differences.

The radiation measurements made in the regions indicated in figure 15 have been compared for the F-1 engine at positions 1 and 5. The spectrometer field of view at the plume used during the tests was approximately 0.8 in. high and 0.25 in. long. No comparisons have been made in the impingement region between engines because methods for predicting the three-dimensional flow field in this region have not yet been perfected.

The predicted flow field properties and radiation for the F-1 engine are compared in figures 16 through 19. The comparisons are excellent except for a slight wavelength discrepancy in the long wavelength channel which is attributed to uncertainty in the data reduction procedure described previously.

IX. CONCLUSIONS

An improved method for calculating radiative heat transfer through inhomogeneous, Saturn-type exhaust plumes, has been developed. This calculation method uses a band model approach in representing the absorption and emission characteristics of the exhaust gases. A modified Curtis-Godson approximation is used in the radiative heat transfer calculations which effectively average the band model parameters over the inhomogeneous path. This technique has been shown to be accurate for strong gradients in temperature and concentration. It has been shown that the difference between the measured inhomogeneous transmittance and that calculated by the modified Curtis-Godson approximation

was within the experimental error and was not greater than .02. These band model parameters should be completely determined by November 1967. An improved set of S/d values have been obtained for H_2O , CO_2 , and CO . A first set of γ/d values have been obtained for these gases. This first set of band model parameters is used in the radiative heat transfer program. At this time very little experimental data are available for comparison with the calculations. As flow field data improve, comparisons between experiment and calculation should be much more favorable. Extensive flow field work is now in progress. Other improvements will come from refined values of the fine structure parameters, particularly the dependence of γ/d on temperature and wave number at long path lengths. The mass absorption coefficient of carbon as a function of frequency and temperature has been determined, using a small perfectly balanced rocket nozzle. These data, along with sampling data, show the carbon to agree with the theory of Stull and Plass. A three-dimensional method of characteristics program and a finite difference technique are being developed to predict gas properties in the impinging regions of the exhaust plumes of the Saturn V.

TABLE 1. FINE STRUCTURE PARAMETERS

Band	Doppler half-width γ_d (cm ⁻¹)	Collision half-width γ_c (cm ⁻¹)	Line Density $\frac{1}{d}$ (cm)
H ₂ O All Bands	$1.39 \times 10^{-6} \bar{\nu}_0 \sqrt{\frac{T}{273}}$ Ref (25)	$P(0.524) \sqrt{\frac{T_0}{T}} \left[\left(\sqrt{\frac{T_0}{T}} + 1 \right) C_{H_2O} + (1 - C_{H_2O})(0.18) \right]$ Ref (3)	$\left[\exp(-0.00106 T + 1.21) \right]^{-1}$ Ref (3)
CO ₂ (4.3 μ)	$0.891 \times 10^{-6} \bar{\nu}_0 \sqrt{\frac{T}{273}}$ Ref (25)	$0.067 P / \sqrt{\frac{T}{273^\circ K}}$ Ref (25, 26)	TABULATED Ref (3)
CO ₂ (2.7 μ)	$0.891 \times 10^{-6} \bar{\nu}_0 \sqrt{\frac{T}{273}}$ Ref (25)	$0.067 P / \sqrt{\frac{T}{273^\circ K}}$ Ref (25, 26)	TABULATED Ref (3)
CO (5 μ)	$1.12 \times 10^{-6} \bar{\nu}_0 \sqrt{\frac{T}{273}}$ Ref (25)	$0.061 P / \sqrt{\frac{T}{273^\circ K}}$ Ref (4)	$\frac{1}{2} \left[3.5961 - 0.0175(\bar{\nu} - 2150) \right]^{-\frac{1}{2}}$ Ref (5)

TABLE II

RANDOM MODEL

P (S)	Emissivity
$\delta(S - S_0)$	$1 - \exp \left[\frac{-2\pi\gamma f(x)}{d} \right]$
$\frac{1}{S_0} e^{-S/S_0}$	$1 - \exp \left[\frac{-S_0 U}{d} \left(1 + \frac{S_0 U}{\pi\gamma} \right)^{-\frac{1}{2}} \right]$
$\frac{1}{INR} S^{-1} \left[\exp \left(-\frac{R-1}{RINR} \right) \right]$	$1 - \exp \left(-\frac{R-1}{INR} \frac{S}{\bar{S}} \right) \frac{\beta_E}{\pi} \left[\left(1 + 2\pi\chi_E \right)^{\frac{1}{2}} - 1 \right]$

WHERE

R is a normalizing factor

$$\beta_E = 2\pi\gamma/d_E$$

$$\chi_E = S_E u / 2\pi\gamma$$

E denotes the mean value

\bar{S} is the mean value

TABLE III

Two-Zone Water Vapor Transmittance at 3990 cm^{-1}

Optical Path: 24" per zone

$$T_1 = T_2 = 1273^\circ\text{K}$$

$$x_1 = x_2 = 3.49$$

$p_1(\text{mm})$	$p_2(\text{mm})$	Measured Transmittance			Calculated $\bar{\tau}$	
		τ_1	τ_2	$\bar{\tau}$	From Eq. (17)	From Eq. (19)
53	53	.720	.729	.621	.628	.634
102	105	.571	.566	.425	.443	.450
150	153	.438	.443	.284	.306	.314
51	104	.743	.571	.515	.524	.530
56	146	.724	.464	.419	.428	.435

TABLE IV

Two-Zone Water Vapor Transmittance at 3990 cm^{-1}

Optical Path: 24" per cone

$$T_1 = T_2 = 637^\circ\text{K}$$

$$x_1 = x_2 = 2.53$$

$p_1(\text{mm})$	$p_2(\text{mm})$	Measured Transmittance			Calculated $\bar{\tau}$	
		τ_1	τ_2	$\bar{\tau}$	From Eq. (17)	From Eq. (19)
51	50	.721	.728	.620	.626	.634
102	100	.510	.528	.368	.384	.395
147	148	.374	.381	.221	.241	.252
148	59	.383	.677	.339	.345	.355
105	49	.513	.726	.462	.468	.477
102	153	.507	.365	.273	.286	.297

TABLE V

Two-Zone Water Vapor Transmittance at 3990 cm^{-1}

Optical Path: 8" per zone

 $T_1 = 1273^\circ\text{K}$ $T_2 = 637^\circ\text{K}$ $x_1 = 1.16$ $x_2 = 0.84$

$P_1(\text{mm})$	$P_2(\text{mm})$	Measured Transmittance			Calculated $\bar{\tau}$		
		τ_1	τ_2	$\bar{\tau}$	From Eq. (17)	From Eq. (19)	From Eq. (18)
50	50	.846	.849	.771	.772	.791	.718
100	100	.744	.728	.617	.619	.648	.542
150	150	.655	.625	.496	.496	.530	.409

TABLE VI

Two-Zone Water Vapor Transmittance at 3990 cm^{-1} $T_1 = 1273^\circ\text{K}$ $T_2 = 637^\circ\text{K}$ $\ell_1 = 8''$ $\ell_2 = 1.5''$ $x_1 = 1.16$ $x_2 = .16$

$P_1(\text{mm})$	$P_2(\text{mm})$	Measured Transmittance			Calculated $\bar{\tau}$	
		τ_1	τ_2	$\bar{\tau}$	From Eq. (17)	From Eq. (18)
50	50	.853	.960	.840	.836	.827
100	100	.751	.923	.723	.720	.682
150	150	.650	.882	.612	.607	.563

TABLE VII

Two-Zone Water Vapor Transmittance at 3990 cm^{-1}

Optical Path: 24" per zone

 $T_1 = 1273^\circ\text{K}$ $T_2 = 637^\circ\text{K}$ $x_1 = 3.49$ $x_2 = 2.53$

$p_1(\text{mm})$	$p_2(\text{mm})$	Measured Transmittance			Calculated $\bar{\tau}$	
		τ_1	τ_2	$\bar{\tau}$	From Eq. (17)	From Eq. (19)
49	53	.745	.711	.622	.630	.638
100	104	.597	.503	.398	.414	.424
151	151	.443	.358	.247	.260	.270
101	51	.573	.722	.501	.518	.525
148	52	.452	.710	.402	.415	.421



FIGURE I LOW ALTITUDE CASE — SATURN I EXHAUST PLUME



FIGURE 2 HIGH ALTITUDE CASE — SATURN I EXHAUST PLUME

120,000 FT. ALTITUDE
OXYGEN/ETHYLENE (C_2H_4)
O/F = 2.25
 P_c = 1105 PSIA

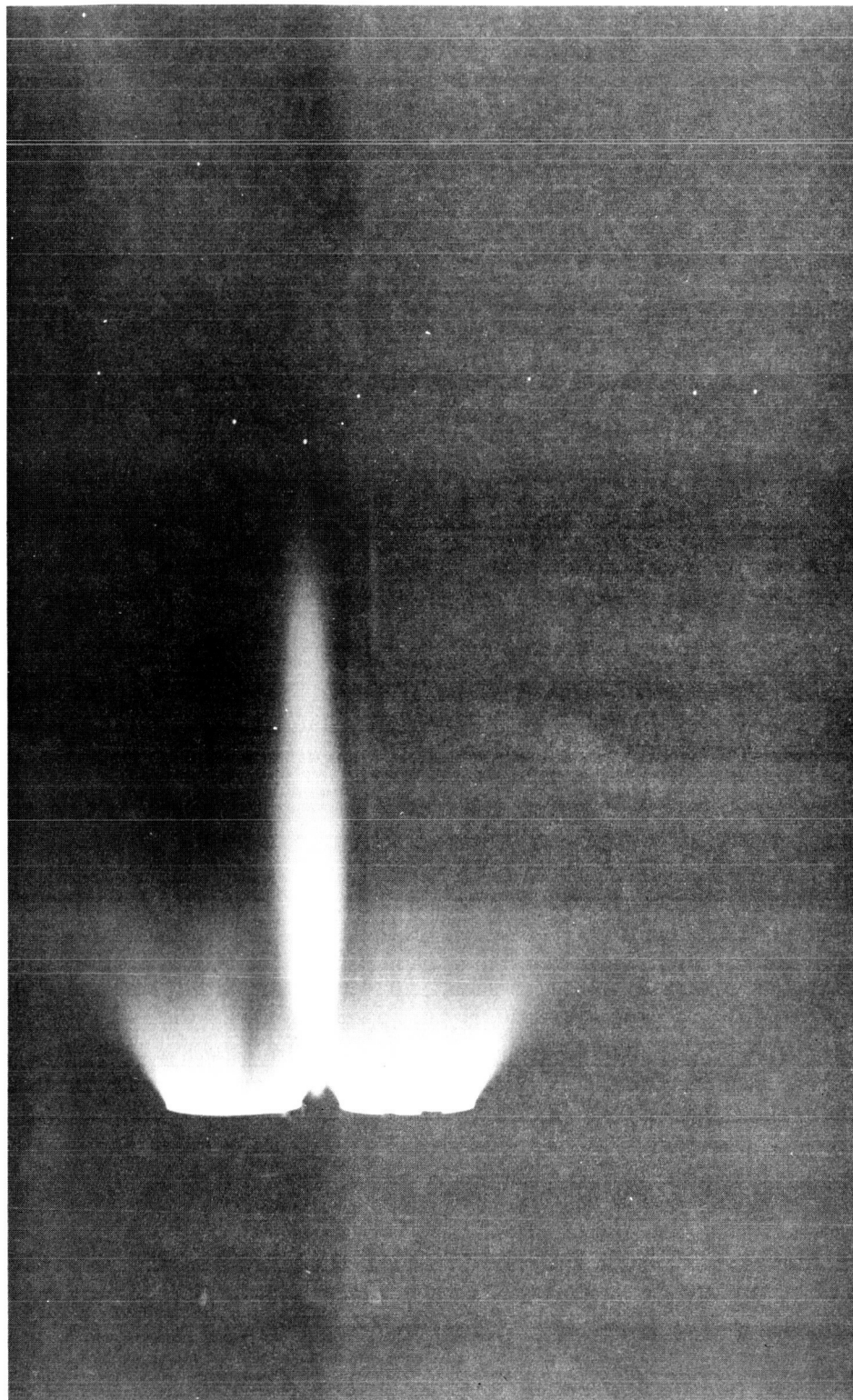


FIGURE 3 1/45 SCALE F-1 ENGINES

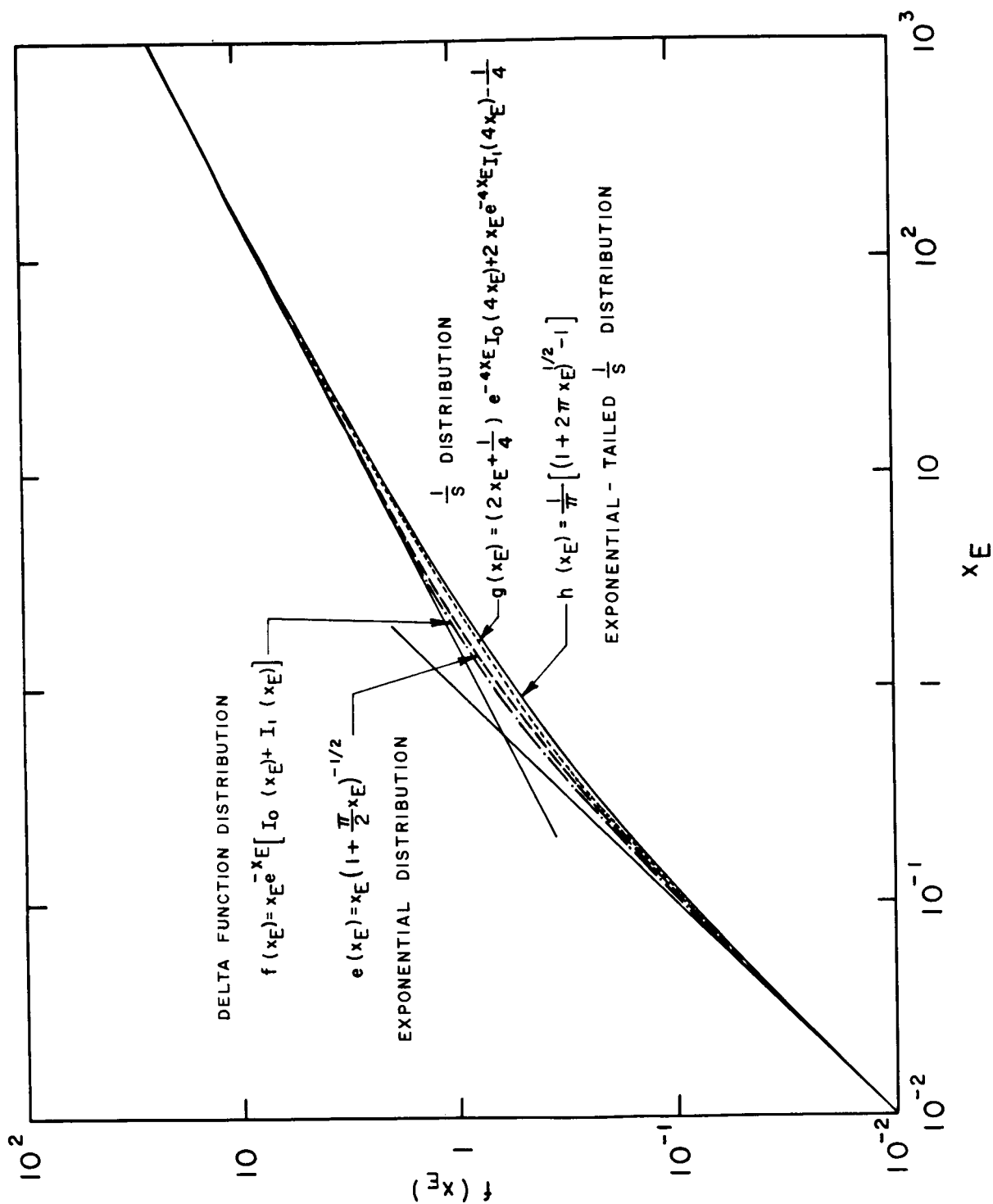


Figure 4 Curves of growth for random band models composed of Lorentz lines for four different intensity distribution functions.

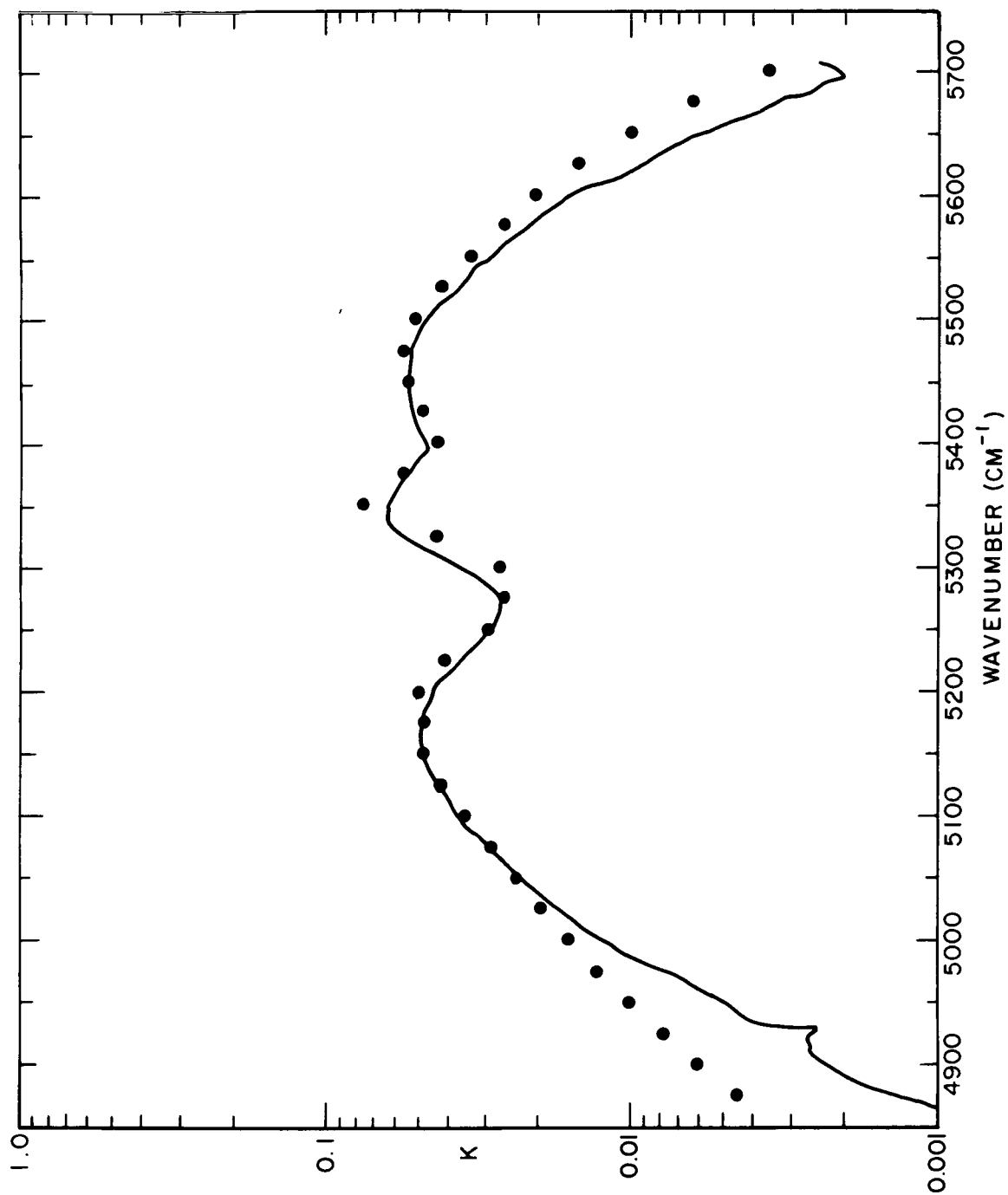


Figure 5 Comparison of absorption coefficients, obtained by Goldstein of the 1.9- μ band at 873°K (solid line). Present values are given as points.

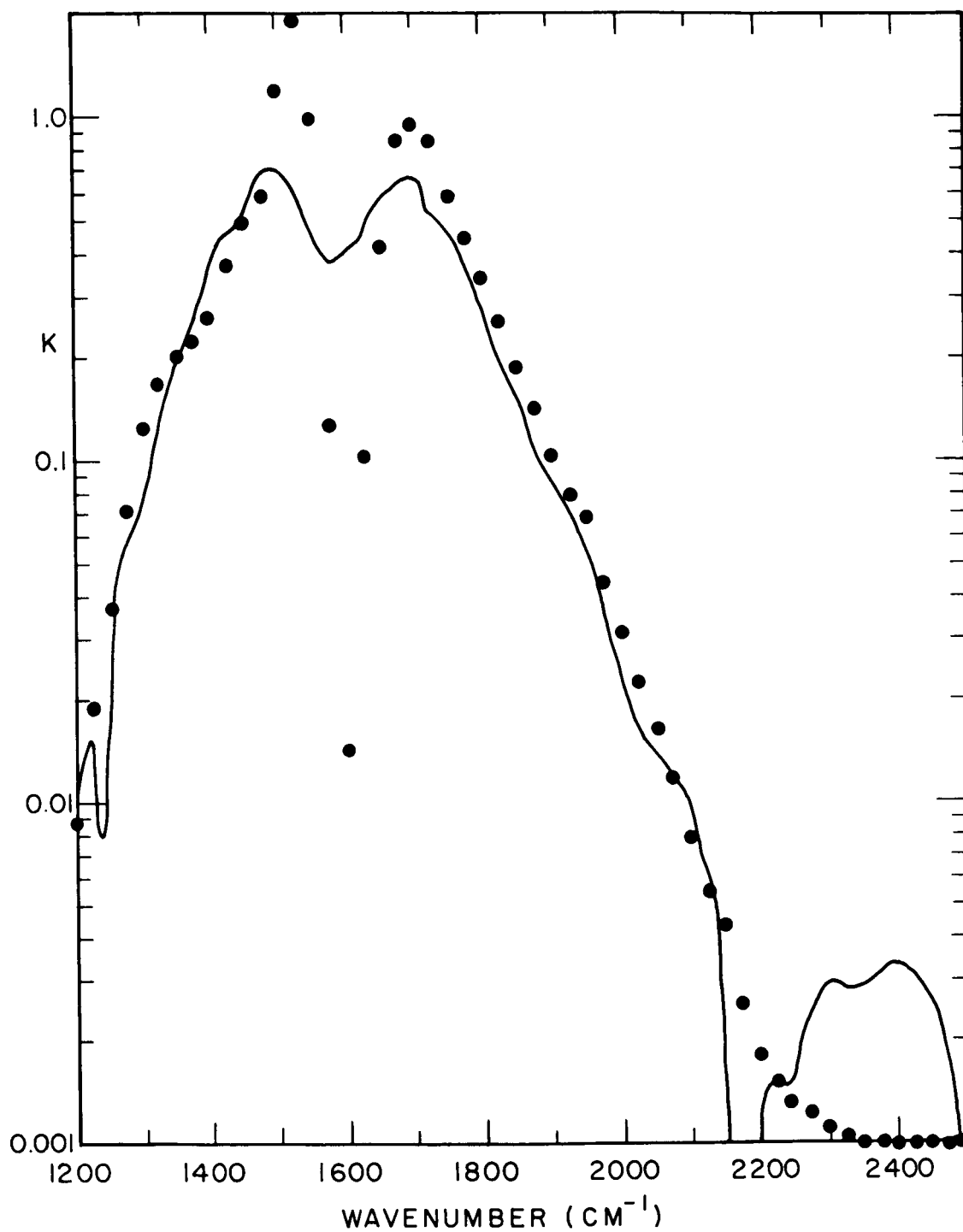


Figure 6 Comparison of absorption coefficients, obtained by Goldstein of the $6.3\text{-}\mu$ band at 473°K (solid line). Present values are given as points.

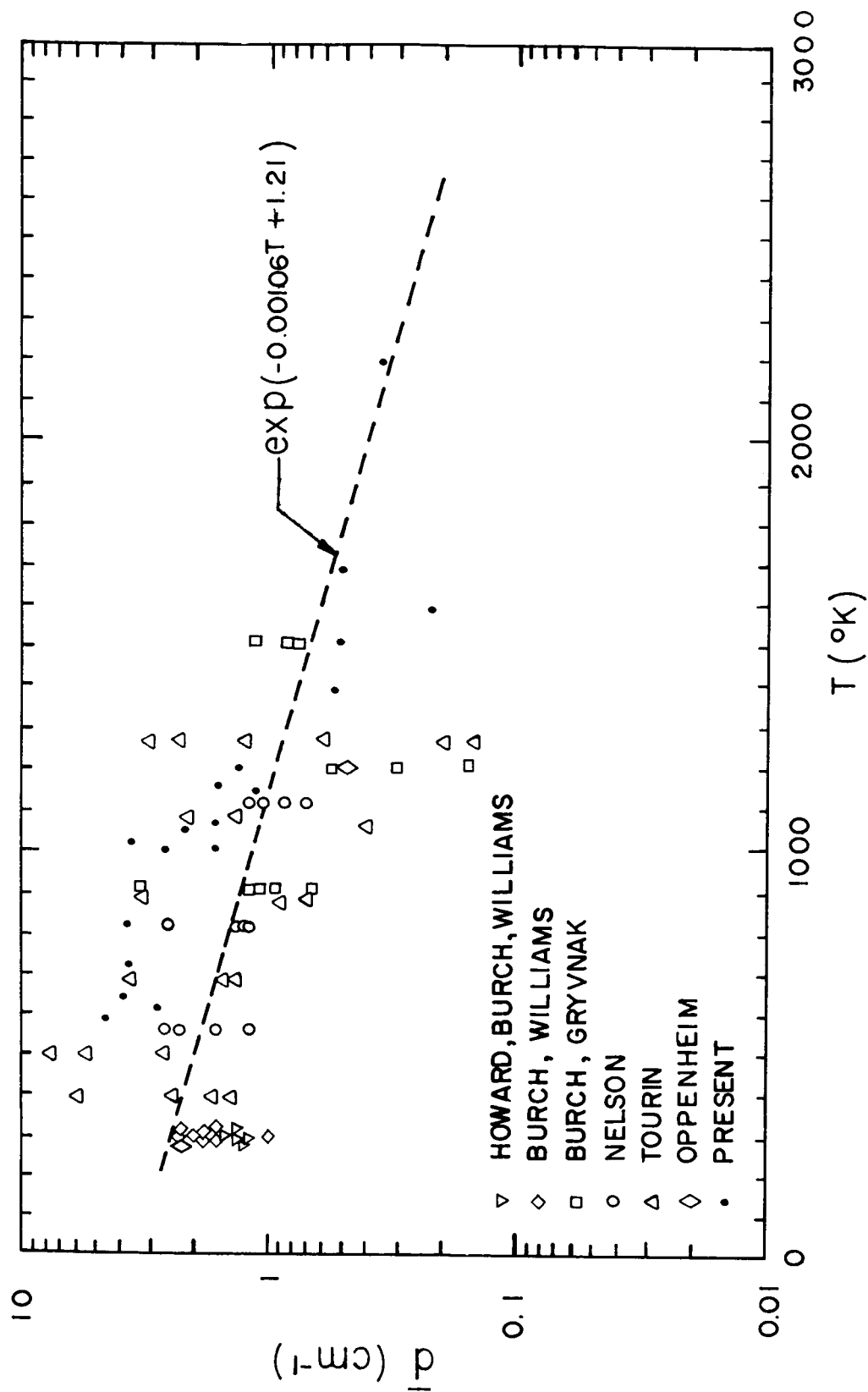


Figure 7. Compilation of band averaged line spacings d versus temperature as obtained from spectra (4.0) taken by several investigators.

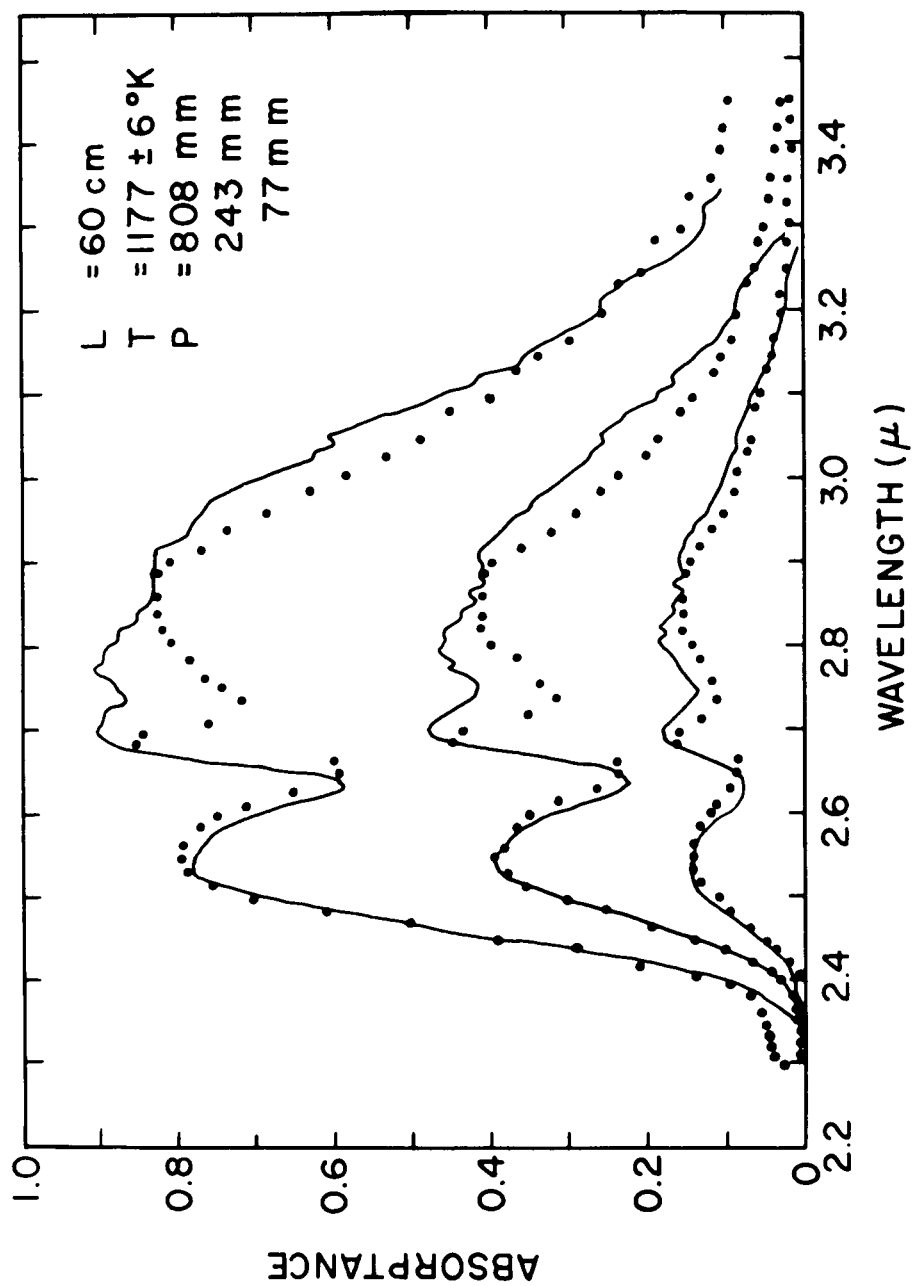


Figure 8 Comparison of measured and calculated emissivity of the 2.7- μ band. Solid lines are the measured spectra taken from Ref. 18, points are the present values.

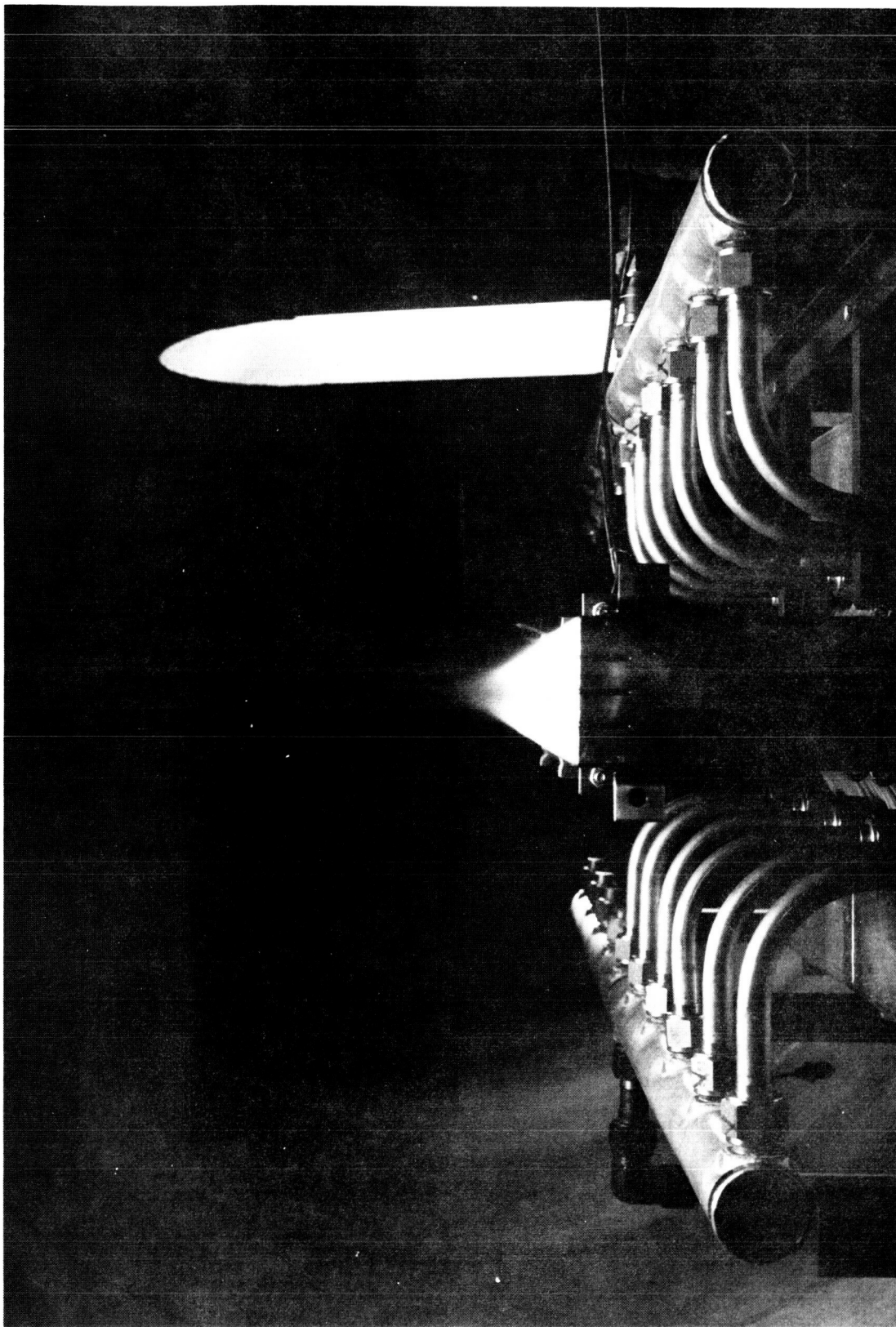


FIGURE 9 END VIEW OF LONG BURNER FLAME

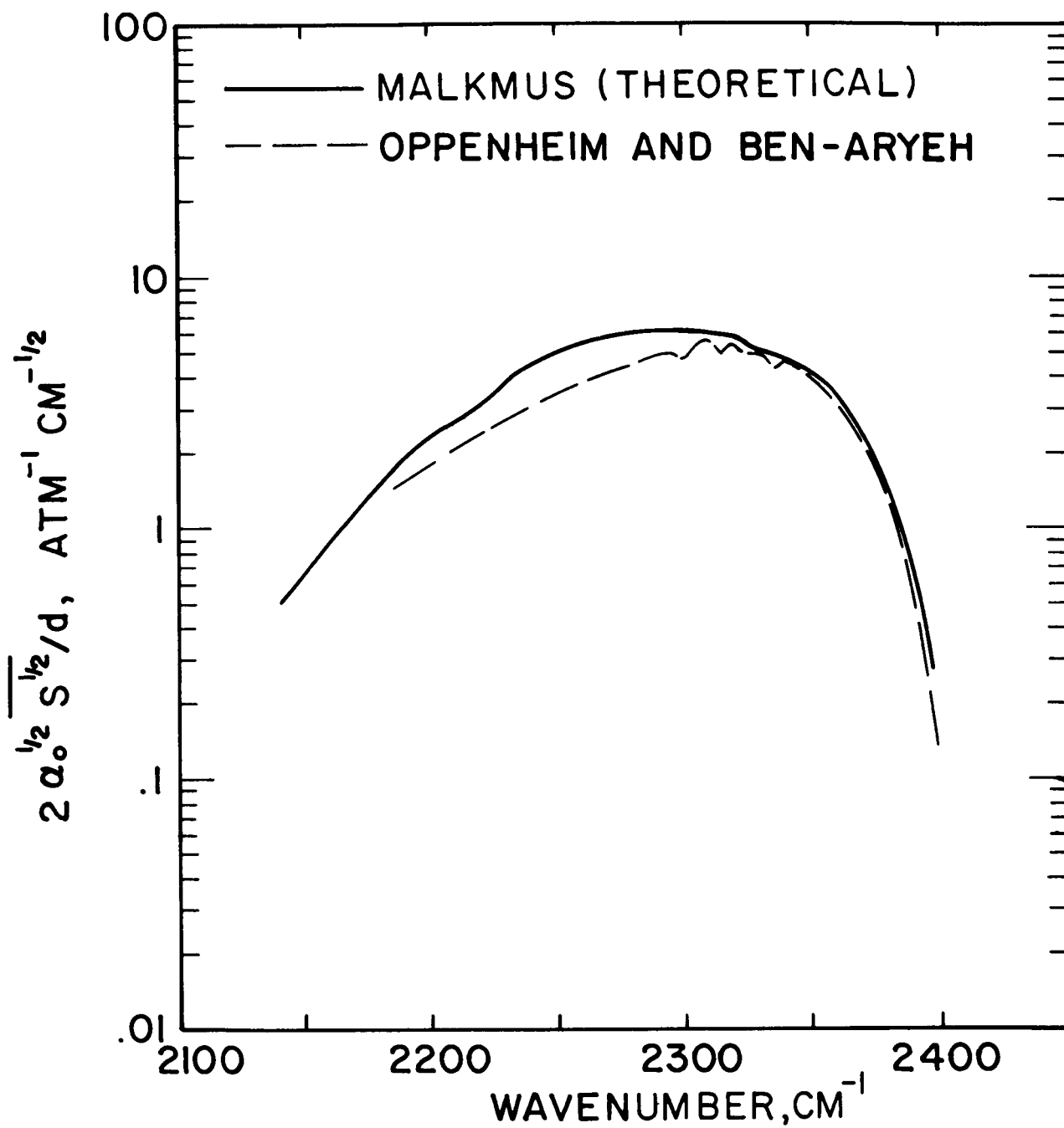


Figure 10 Comparison of theoretical and experimental values of $2\alpha_0^{1/2} S^{1/2}/d$
(taken from Reference)

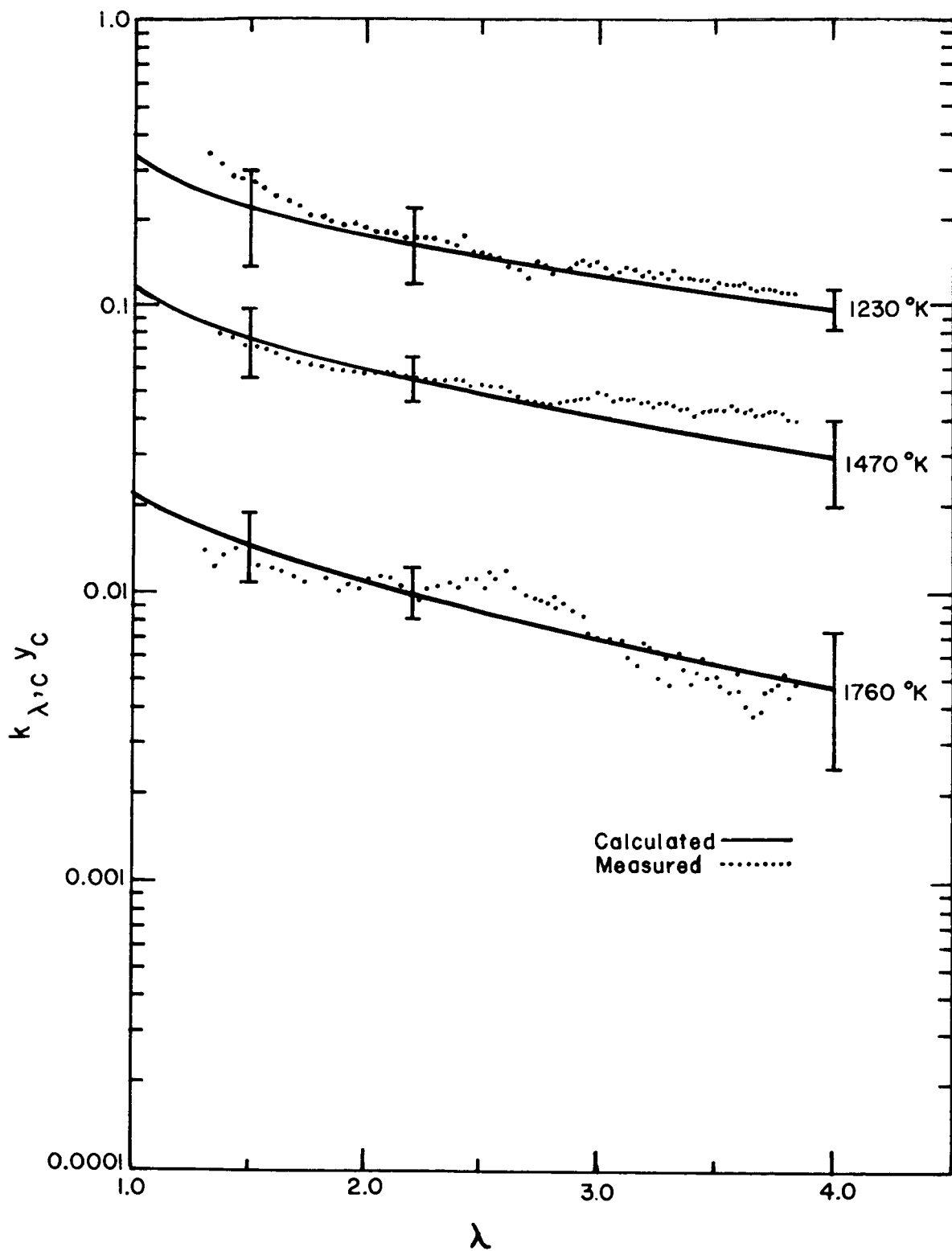


FIGURE II. ABSORPTION COEFFICIENT X MASS FRACTION VERSUS WAVELENGTH FOR CARBON PARTICLES AT VARIOUS TEMPERATURES

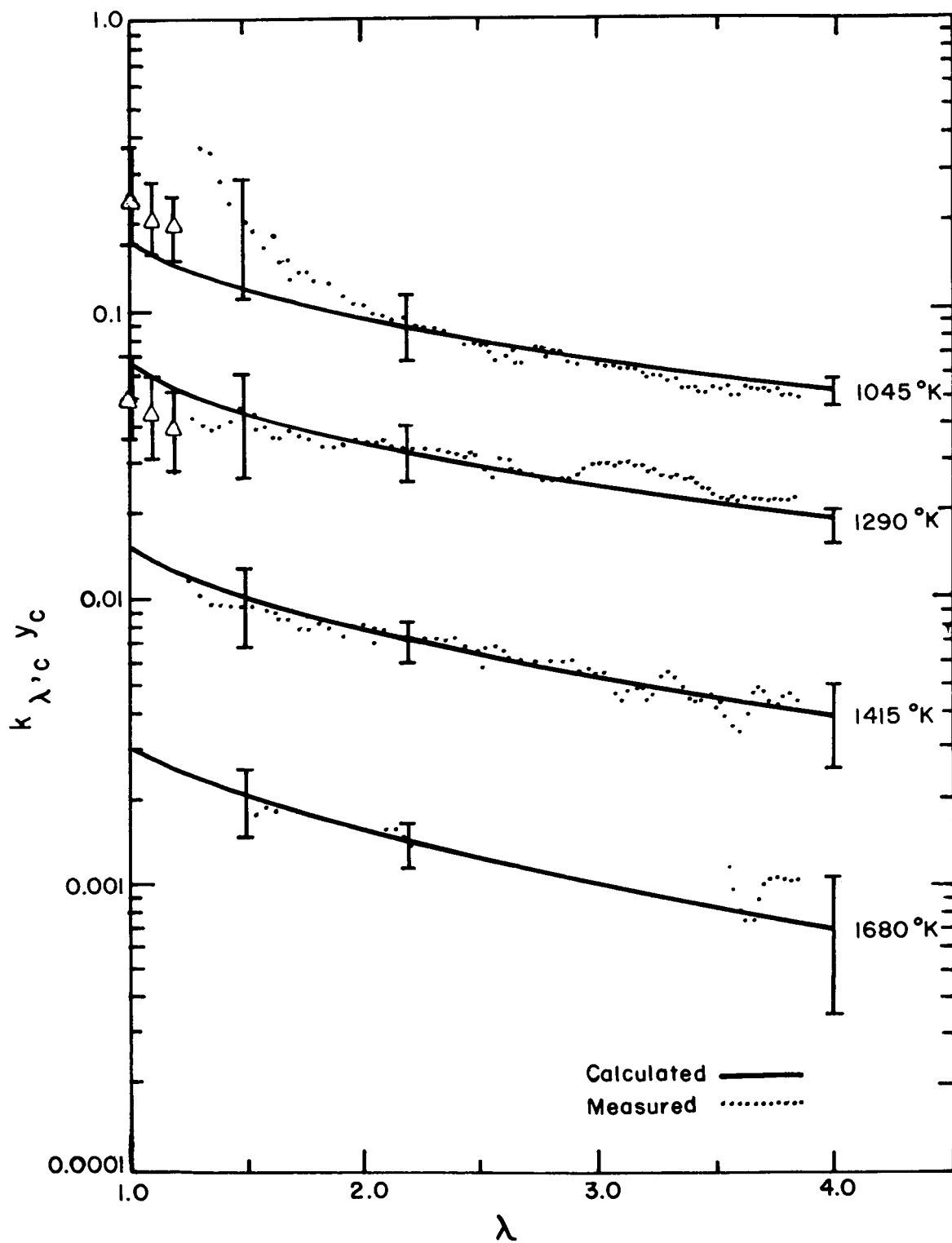


FIGURE 12. ABSORPTION COEFFICIENT X MASS FRACTION
VERSUS WAVELENGTH FOR CARBON PARTICLES
AT VARIOUS TEMPERATURES



**FIGURE 13 ELECTRON MICROGRAPH COLLECTED SOOT
PARTICLES-TEST MAGNIFICATION 96500X**

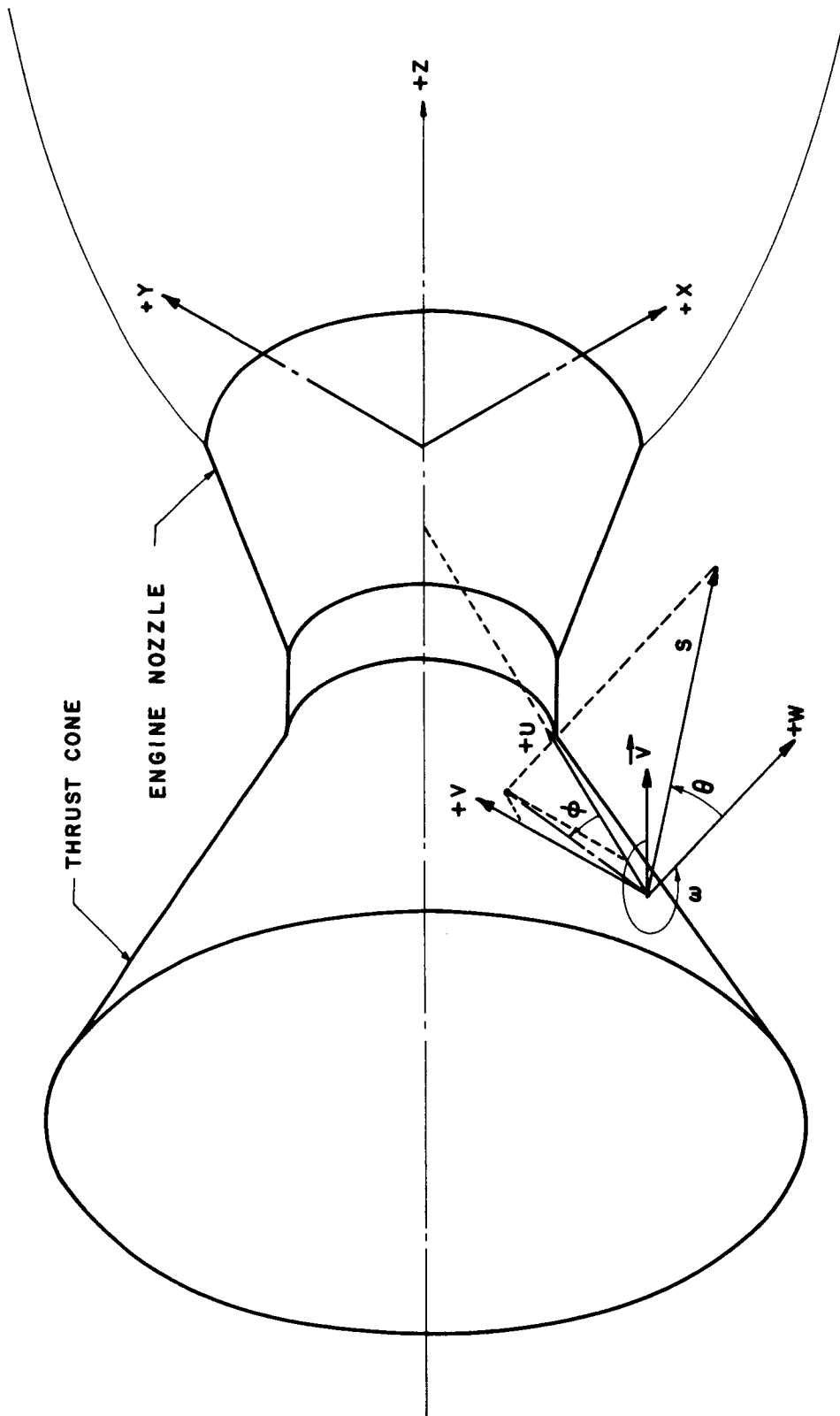


FIGURE 14 ILLUSTRATION OF COMPUTER PROGRAM GEOMETRY

F-1 ENGINE — NOMINAL OPERATING CONDITIONS

ALTITUDE — 120,000 ft
 COMBUSTION CHAMBER PRESSURE — 1000 psia
 MIXTURE RATIO — $O/F = 2.25$ (O_2/C_2H_4)
 MEASUREMENT POSITION — 1
 NO. OF ENGINES OPERATING — 2

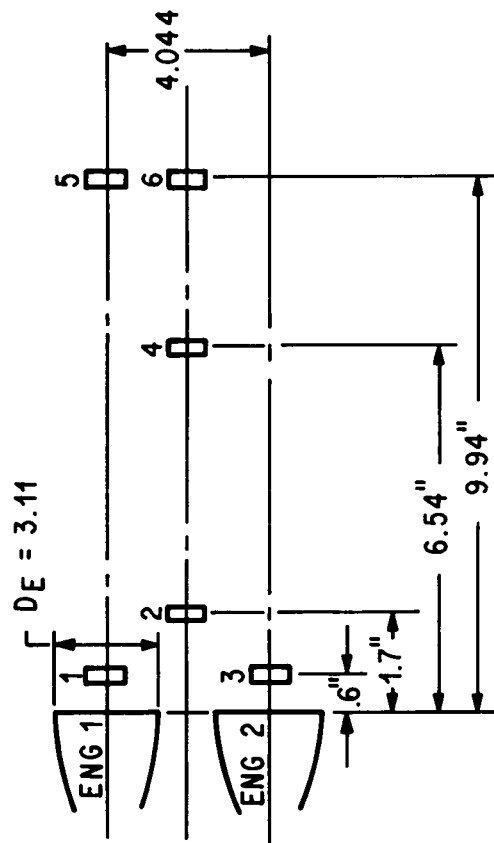


FIG. 15. TEST SUMMARY-TWO-ENGINE PLUME RADIATION STUDY

Properties Predicted for O_2/C_2H_4 Propellants, $O/F = 2.25$,
 $P_c = 1000$ psia, $P_\infty = 9.61$ psfa, and Equilibrium Composition
 During Expansion.

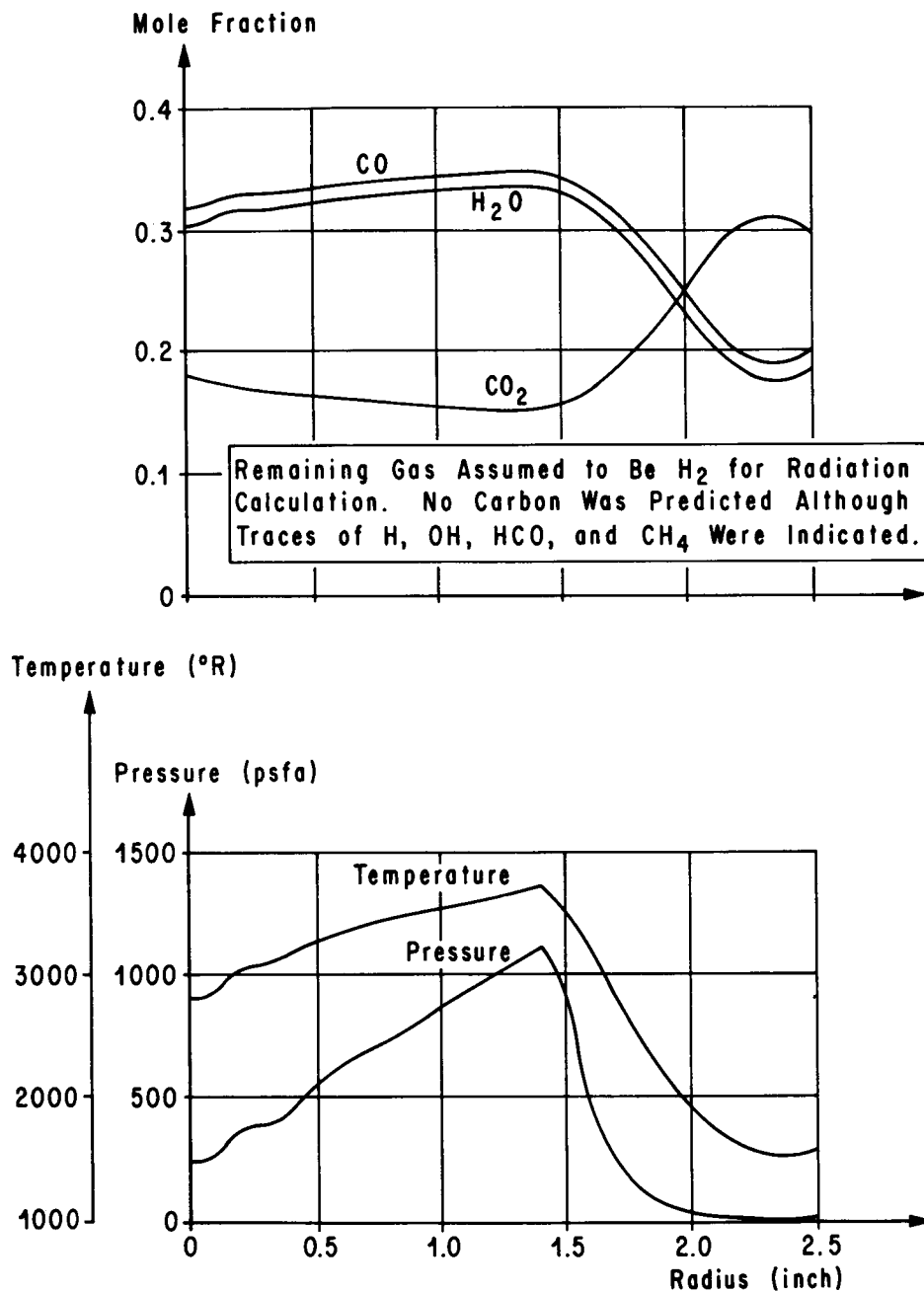


FIG. 16. PREDICTED PROPERTY VARIATIONS
 0.6 INCHES DOWNSTREAM OF A 1/45 SCALE F-1 ENGINE EXIT

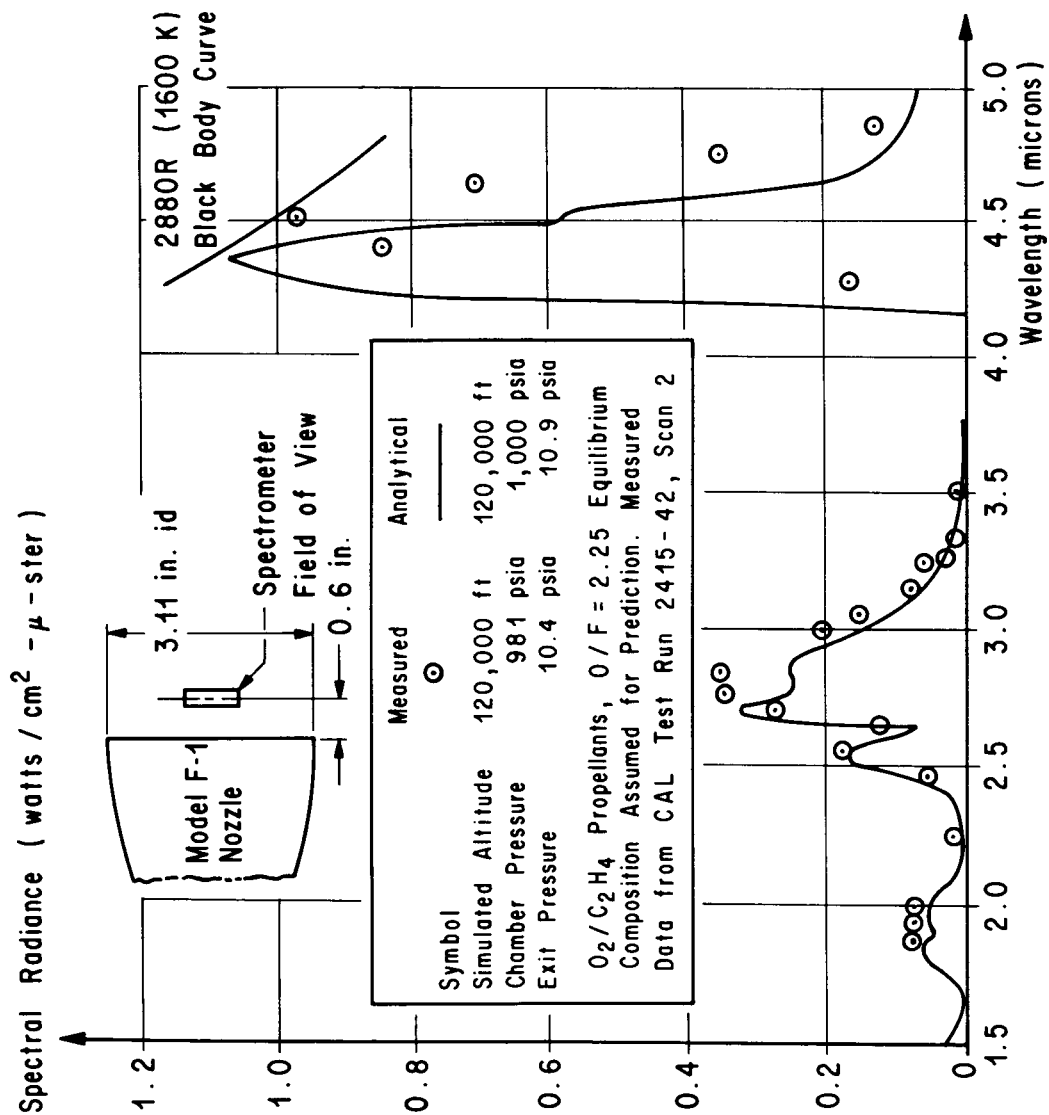


FIG. 17. COMPARISON OF MEASURED AND PREDICTED RADIATION
NEAR THE EXIT OF A 1/45 SCALE F-1 ENGINE

Properties Predicted for O_2/C_2H_4 Propellants,
 $O/F = 2.25$, $P_c = 1000$ psia, $P_\infty = 9.61$ psfa,
 and Equilibrium Composition During Expansion.

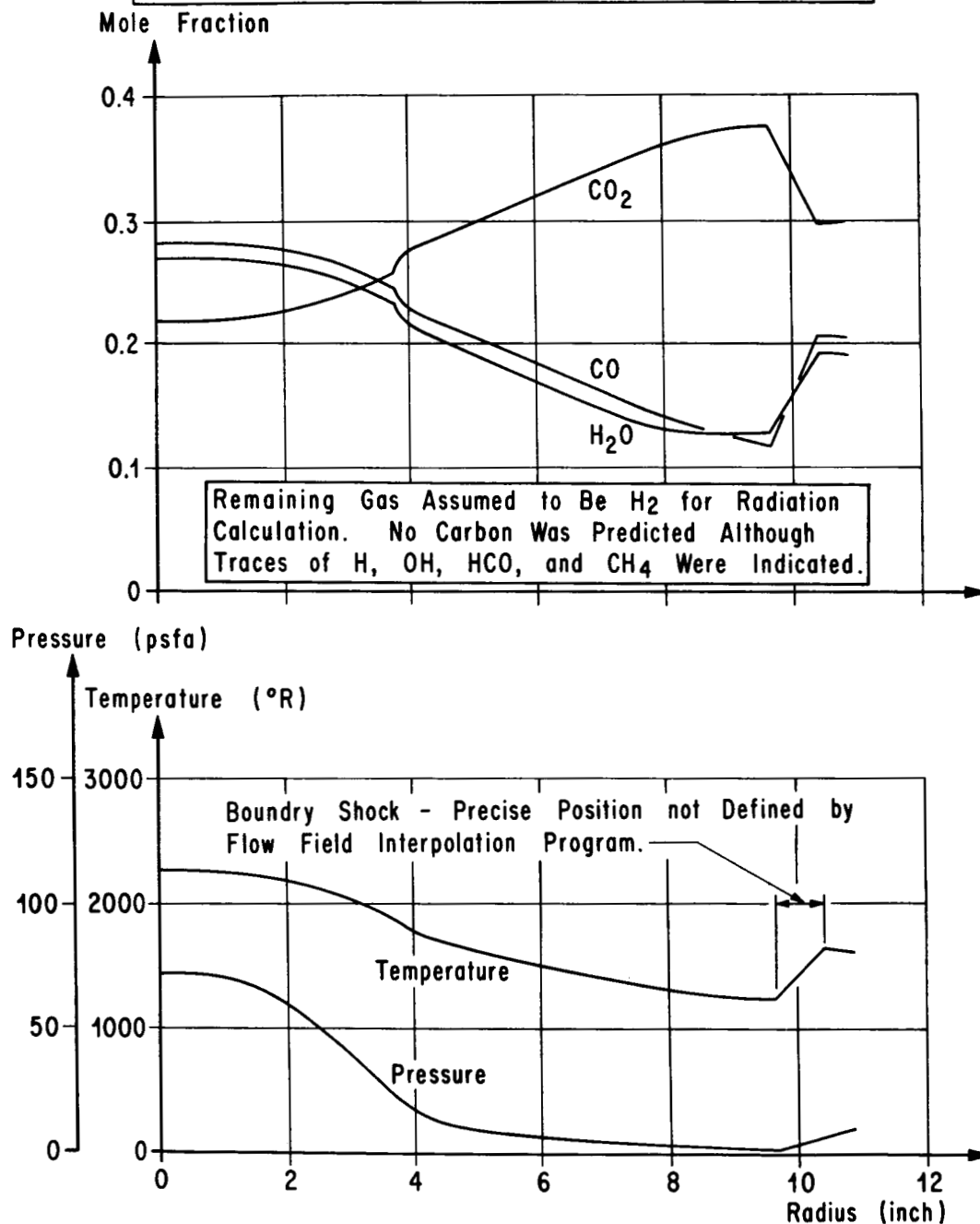


FIG. 18. PREDICTED PROPERTY VARIATIONS
 9.94 INCHES DOWNSTREAM OF A 1/45 SCALE F-1 ENGINE EXIT

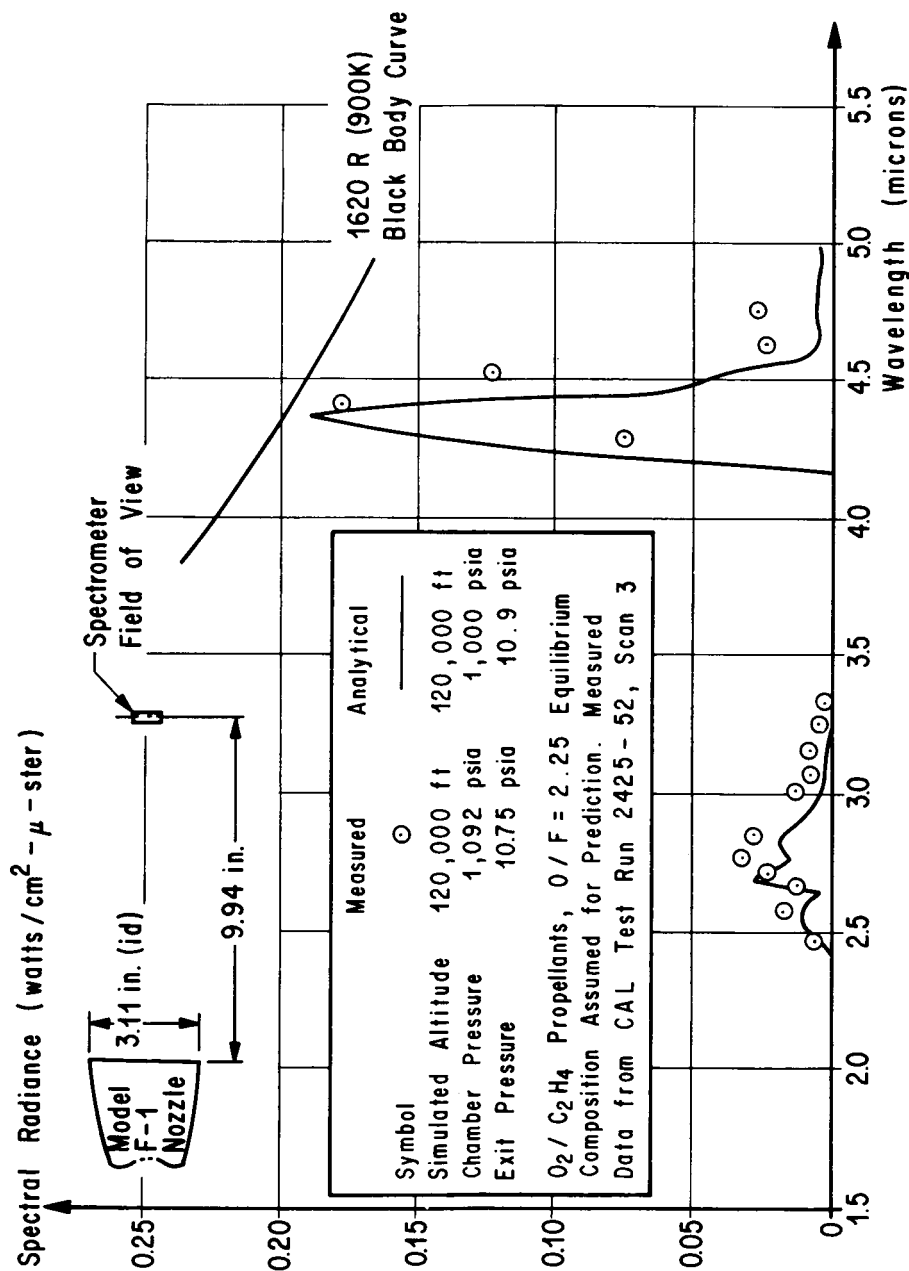


FIG. 19. COMPARISON OF MEASURED AND PREDICTED RADIATION
 9.94 INCHES AFT OF THE EXIT OF A 1/45 SCALE F-1 ENGINE

REFERENCES

1. Dahm, W. K., "Present Techniques and Problems in the Determination of the Base Heating Environment of Propelled Boost and Space Vehicles," International Symposium on Space Technology and Science, 5th, Tokyo, Japan, A65-14290 05-31, September 2-7, 1963.
2. Powers, S. A. and H. Ziegler, "Determination of the Aerodynamic Properties of Engine Exhaust Plumes," Northrop Corporation, Norair Division, MSFC Contract NAS8-11260.
3. "Study on Exhaust Plume Radiation Predictions," Final Report, General Dynamics/Convair, December 1966, Contract NAS8-11363.
4. Benedict, W. S., Herman, R., Moore, G. E., and Silverman, S., *Astrophys. J.* 435, 277, (1962).
5. Mayer, H., "Methods of Opacity Calculations," Los Alamos Report No. LA-647 (Oct. 47).
6. Goody, R. M., "A Statistical Model for Water Vapor Absorption," *Quart. J. Roy. Met. Soc.* 78, 165, (1952).
7. Krakow, B., Babrov, H. J., Maclay, G. J., and Shabott, A. L., "Use of Curtis-Godson Approximation in Calculation of Radiant Heating by Inhomogeneous Hot Gases," NASA TM X-53411.
8. Plass, G. N., "Useful Representations for Measurements of Spectral Band Absorption," *J. Opt. Soc. Am.* 50, 868, (1960).
9. Malkmus, W., *J. Opt. Soc. Am.* 53, 951 (1963).
10. Malkmus, W., *J. Opt. Soc. Am.* 54, 751 (1964).
11. Malkmus, W., Thomson, A., *J. Quant. Spect. Rad. Transfer* 2, 17 (1962).
12. Ferriso, C. C., *J. Chem. Phys.* 37, 1955 (1962).
13. Ferriso, C. C., Ludwig, C. B., *J. Opt. Soc. Am.* 54, 657 (1964).
14. Stull, V. R., Plass, G. N., "Emissivity of Dispersed Carbon Particles," *J. Opt. Soc. Am.* 50, 121-129 (1960).
15. Benedict, W. S., et al., *Can. J. Phys.* (34), 830, (1956).
16. Plass, G. N., "The Theory of the Absorption of Flame Radiation by Molecular Bands," *Appl. Opt.* 4, 161, (1965).

REFERENCES (Continued)

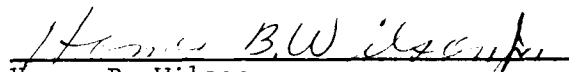
17. Plass, G. N., "Spectral Band Absorptance of Radiation Traversing Two or More Cells in Series," Appl. Opt. 4, 69 (1965).
18. Simmons, F. S., Arnold, C. B., and Kent, N. F., "Studies of Infrared Radiative Transfer in Hot Gases, Nonisothermal Radiance Measurements in the 2.7 H₂O Bands," BAMIRAC 4613-93-T, December 1965.
19. Oppenheim, U. P., Goldman, A., "Spectral Emissivity of Water Vapor at 1200°K," Tenth Symposium (International) on Combustion 10, 185, The Combustion Institute (1965).
20. Ferriso, C. C., Ludwig, C. B., and Action, L., "Spectral Emissivity Measurements of the 4.3 CO₂ Band Between 2650 and 3000°K," GD/C-DBE 65-017, August 1965.
21. Oppenheim, U. P., Ben-Aryeh, Y., "Statistical Model Applied to the Region of the ν_3 Fundamental of CO₂ and 1200°K," J. Opt. Soc. Am., 53, 344, 1963.
22. Ferriso, C. C., Ludwig, C. B., "Spectral Emissivities and Integrated Intensities of the 1.87, 1.38, and 1.14 Micron H₂O Bands Between 1000 and 2200°K," J. Chem. Phys. 41, 1668, 1964.
23. Penzias, G. J. and Maclay, G. J., "Analysis of High Temperature Gases in Situ by Means of Infrared Band Models," NASA CR-54002.
24. Tourin, R. H., "Spectral Emissivities of Hot CO₂-H₂O Mixtures in the 2.7 μ Region," J. Opt. Soc. Am. 51, 799, 1961.
25. Goody, R. M., Atmospheric Radiation I. Theoretical Basis, Oxford (1964).
26. Kaplan, Lewis D., and Eggers, David F., "Intensity and Line Width of the 15 Micron CO₂ Band Determined by a Curve of Growth Method," J. Chem. Phys., p. 876, 1956.
27. Prozan, R. J., "Development of a Method of Characteristics Solution for Supersonic Flow of an Ideal, Frozen, or Equilibrium Reacting Gas Mixture," LMSC/HREC A782535, April 1966.


INHOMOGENEOUS RADIANT HEAT TRANSFER FROM SATURN ROCKET EXHAUST PLUMES


by Robert M. Huffaker

The information in this report has been reviewed for security classification. Review of any information concerning Department of Defense or Atomic Energy Commission programs has been made by the MSFC Security Classification Officer. This report, in its entirety, has been determined to be unclassified.

This document has also been reviewed and approved for technical accuracy.


Homer B. Wilson
Chief, Thermal Environment Branch


Werner K. Dahm
Chief, Aerophysics Division


E. D. Geissler
Director, Aero-Astroynamics Laboratory

DISTRIBUTION

DEP-T	Sci. & Tech. Info. Facility (25)
	P. O. Box 33
MS-IP	College Park, Md.
	Attn: NASA Rep. (S-AK/RKT)
MS-IL (8)	
	Chrysler Corp. Space Div.
CC-P	P. O. Box 26018
	New Orleans, La. 70129
I-RM-M	Attn: Mr. B. Elam
	Mr. D. Thibodeaux
MS-H	Mr. R. Taylor
MS-T (6)	
	Hayes International Corp.
	P. O. Box 2287
HME-P	Birmingham, Ala. 35201
	Attn: Mr. John Reardon
<u>R-P&VE</u>	
Dr. Lucas	North American Aviation
Mr. Goerner	Rocketdyne Division
Mr. Kannan	6633 Canoga Ave.
Mr. McKay	Canoga Park, Calif.
Mr. Paul	Attn: Mr. S. Golden
Mr. Wood	Mr. J. Muirhead
	Mr. J. Hon
R-TEST (5)	
	The Warner & Swasey Co.
R-RP (5)	Control Instrument
	32-16 Dowing St.
<u>R-AERO</u>	Flushing, N. Y. 11354
Dr. Geissler	Attn: Mr. R. Tourin
Mr. Murphree	Mr. H. Babrov
Mr. Dahm	
Mr. Wilson	General Dynamics/Convair
Dr. Farmer	5001 Kearney Villa Rd.
Mr. Huffaker	San Diego, Calif. 92112
Mr. Brewer	Attn: Mr. K. Ludwig
Mr. Dash	Mr. F. Boynton
Miss Forbush	Mr. Thomson
Mr. Horn	
Mr. W. Vaughan	
Mr. Lindberg	
Mr. Thomae	
Dr. H. Krause	
Mr. Baker	

DISTRIBUTION (Continued)

Mr. Peter A. Cerreta
Code RV-1
NASA Headquarters
Independence Ave.
Washington, D. C. 20546

Dr. Robert Boulard
School of Engineering & Aeronautical Sciences
Purdue University
LaFayette, Indiana

Dr. James C. Wu
School of Aerospace Engineering
Ga. Inst. of Tech.
Atlanta, Ga. 30332

Mr. King Bird
Cornell Aeronautical Laboratory, Inc.
Cornell University
Buffalo, New York

Dr. Kenneth R. Purdy
Sch. of Mech. Engr.
Purdue Univ.
LaFayette, Ind. 47907

Dr. B. F. Barfield
Mechanical Engineering Department
Box 1972
Univ. of Ala.
University, Alabama 35486

Mr. Joseph M. O'Byrne
Dept. of Mech. Engr.
Univ. of Mass.
Amherst, Mass. 01002